Using Multilayer Heterogeneous Networks to Infer Functions of Phosphorylated Sites

*Joanne Watson[1, 2], Jean-Marc Schwartz[1] and Chiara Francavilla[2]**

* Corresponding Author: chiara.francavilla@manchester.ac.uk

[1]Division of Evolution & Genomic Sciences, School of Biological Sciences, Faculty of Biology, Medicine & Health, University of Manchester, Manchester, M13 9PT

[2]Division of Molecular and Cellular Function, School of Biological Sciences, Faculty of Biology, Medicine & Health, University of Manchester, Manchester, M13 9PT.

1. Abstract

Mass spectrometry-based quantitative phosphoproteomics has become an essential approach in the study of cellular processes such as signaling. Commonly used methods to analyze phosphoproteomics datasets depend on generic, gene-centric annotations such as Gene Ontology terms which do not account for the function of a protein in a particular phosphorylation state. Analysis of phosphoproteomics data is hampered by a lack of phosphorylated site-specific annotations. We propose a method that combines shotgun phosphoproteomics data, protein-protein interactions, and functional annotations into a heterogeneous multilayer network. Phosphorylation sites are associated to potential functions using a random walk on heterogeneous network (RWHN) algorithm. We validated our approach against a model of the MAPK/ERK pathway and functional annotations from PhosphoSite Plus and were able to associate differentially regulated sites on the same proteins to their previously described specific functions. We further tested the algorithm on three previously published datasets and were able to reproduce their experimentally validated conclusions and to associate phosphorylation sites with known functions based on their regulatory patterns. Our approach provides a refinement of commonly used analysis methods and accurately predicts context-specific functions for sites with similar phosphorylation profiles.

Keywords: phosphoproteomics, functional analysis, bioinformatics, multilayer networks, random walk, gene ontology, pathways

2. Introduction

Phosphorylation is the most studied post-translational modification (PTM) due to its central role in cellular regulation. It is thought to be the principal PTM in the human proteome, as well as an essential mediator of protein-protein interaction (PPI) and protein function [1]. Transient changes occur at specifically regulated phosphorylation sites, of which there may be multiple on each protein. Regulation of phosphorylation is often dependent on perturbations such as the activity of extracellular ligands, drug treatment or physical stimuli in the extracellular environment [2]. By comparing changes in the phosphoproteome of cells in different experimental conditions through mass spectrometry-based phosphoproteomics, phosphorylated sites that are key players in cellular processes and functions can be uncovered in an unbiased, high-throughput manner [3].

Functional analysis of phosphoproteomics datasets is typically based on gene-centric enrichment of Gene Ontology (GO) terms or involvement in known pathways [4]. However, this approach disregards information captured by phosphoproteomics data on changes at specific phosphorylated sites, by limiting the analysis to the protein level. The modification state of a protein is inherently coupled to its function; PTMs alter protein activity, as well as the ability to interact with different sets of proteins. Furthermore, if a protein is phosphorylated on multiple sites, each with a different function and regulatory pattern, this information is not revealed by gene-centric analysis [5]. For instance, the well-studied signalling protein MAPK1 has 18 known phosphorylated sites recorded in the database PhosphositePlus® (PSP), however only 6 have been annotated to a downstream function[6]. In the most recent release of PSP (v6.5.9.3), only 4271 of the more than 230,000 human phosphorylated sites recorded in the database are associated to 19 generic biological functions (e.g., “cell cycle”, “transcription”), which are qualified with one of: “induced”, “inhibited”, “regulated” or “altered”. Enrichment analyses that rely on generalizations based on protein-level or gene-centric descriptions exclude the details that are encoded in the phosphorylation

signature. Analyses are thus hampered by the lack of phosphorylation site-specific functional annotations.

Several network-based methods have been proposed to move towards phosphorylation site-specific analyses of phosphoproteomics data. A significant focus has been on the inference of kinase-substrate networks, such as NetworKIN [7], KSEA [8], and IKAP [9], among others. These methods are useful for reconstructing the architecture of signalling intracellular networks, which can be informative for identifying modules of modified proteins involved in cellular processes, but again remain hampered by the lack of site-specific functional annotation [10]. They may also be biased towards the most studied kinases and the exclusion of non-kinase proteins. Rudolph *et al.* [11] proposed a method to address this issue named PHOTON which identified differentially regulated proteins based on the level of phosphorylation of their binding partners in a high-confidence PPI network, and then used logistic regression to identify the involvement of the phosphorylated proteins in known signalling pathways. PHOTON is not truly site-centric, however, as it relies on summarized quantitative values of phosphorylated sites. An alternative approach described by Krug *et al.* [12] uses a modification to the gene-centric method gene set enrichment analysis (GSEA), which relies on a curated resource containing literature-derived phosphorylated site-specific signatures to assign functions to sites. However, the use of such a resource is limited by the lack of phosphorylated-site annotation to these signatures or specific cellular processes; though useful for identifying well-studied sites, predictions of functions of under-studied or sites in alternative contexts would not be captured. These do not fulfil the same role as popular gene-centric methods such as over-representation analysis (ORA)[13] in aiding prediction and hypothesis generation when performing exploratory analysis of shotgun phosphoproteomics data.

In recent years, heterogeneous or multilayer networks have been used to represent many types of 'omics datasets [14]. These specialized networks are used to describe multiple types of associations with nodes representing different entities. To identify relationships between the different biological layers, random walk algorithms have been applied to these networks. The random walk on heterogeneous network (RWHN) with restart (RWR) method [15] has been particularly popular. Jiang [16] used RWR to prioritize disease candidate genes in a PPI-phenome network; similarly, Soul *et al*. [17] applied it to a PPI-phenome network to identify disease mechanisms. Recent work has extended the method to multiple layers of biological information, for example to infer disease associated m6A RNA methylation via known gene-disease associations [18]. Similar methodology was used to associate phosphorylation sites recorded in the PSP database to diseases via kinase-substrate interactions [19].

Here, we propose an algorithm that uses RWHN to associate phosphorylated sites to context-specific function via a heterogeneous multilayer network using shotgun phosphoproteomics data. The network combines three layers of information: phosphorylated sites, protein interactions and GO terms. Clustering of phosphoproteomics data is used to find common features within datasets and is generally followed by enrichment analyses. This is based on the assumption that common patterns of phosphorylation, based on temporal changes or in response to a particular stimulus, treatment or environmental context, are a likely indicator of involvement in common functions or processes [20]. We utilize this concept in our algorithm by connecting phosphorylated sites that have been clustered together, and therefore share regulatory patterns, within the multilayer network. The algorithm is intended for use on large phosphoproteomics datasets, assessing perturbations or processes as opposed to an interpretation of the full phosphoproteomics network in the cell.

We first apply our algorithm to a small-scale, manually curated validation network. We also assess the ability of our method and the most commonly used alternative, ORA, to capture the functional descriptions recorded in PSP, which are based on experimental analysis. We then demonstrate the utility of our algorithm using three previously published shotgun phosphoproteomics datasets, describing early signalling events in HeLa cells upon EGF and TGF-α stimulation [21], phosphorylation-mediated changes in breast cancer cells resistant to lapatinib treatment [22] and subcellular location dependent signalling events downstream of HRAS [23], respectively. We demonstrate that phosphorylated sites can be differentially assigned to functional annotations and this is driven by changes in the context-dependent modification of these sites. Our method is suitable for use with any phosphoproteomics dataset and could be generalized for data describing other PTMs.

3. Experimental Procedures

A multilayer heterogeneous network was constructed to relate biological function to phosphorylation sites via a protein-protein interaction network (Figure 1). Three types of nodes are contained within the network: phosphorylation sites (called 'sites' here on in for brevity), proteins and functional annotations (either Gene Ontology Biological Process (GOBP) terms or KEGG pathways). The edges describe five possible associations which are either bipartite (i.e., site to protein, protein to function) or between the same type of node.

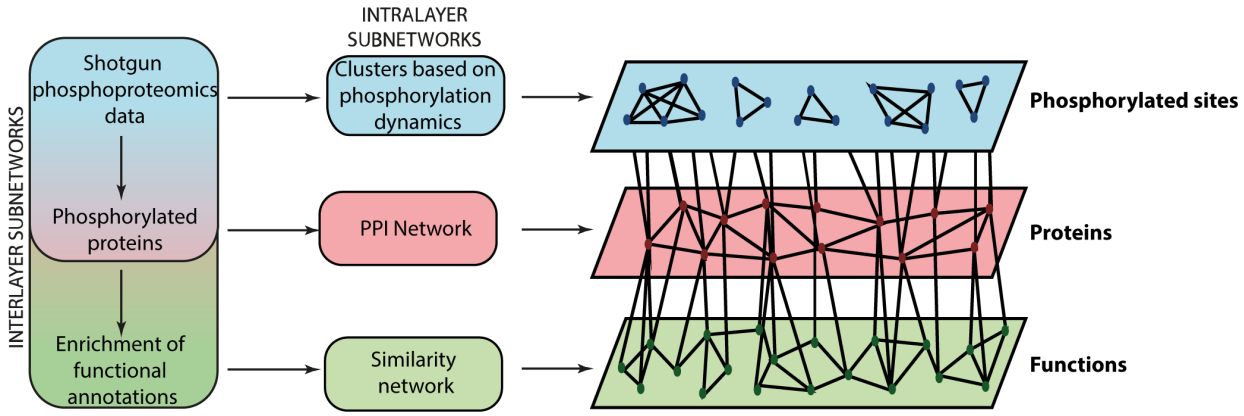

Figure 1. Overview of multilayer heterogeneous network construction from phosphoproteomics data.

Dataset Accession and Processing

Sites annotated to have a role in biological processes were extracted from the `Regulatory sites` dataset, available for download from PhosphoSitePlus® (version 6.5.9.3). The dataset was filtered on the "ON_PROCESS" column to only include sites annotated to biological roles, rather than molecular or interaction roles.

The results of the phosphoproteomics experiment described in Francavilla *et al.* [21] were taken from Supplementary Table S1 of their manuscript. The authors had processed the raw mass spectrometry data using MaxQuant [24], filtered identified phosphorylated sites based on a localization probability of greater than 0.75 and normalized remaining data to the ratio of EGFR at 1 min after stimulation with EGF or TGF-α. Prior to multilayer heterogeneous network construction, the data were further filtered to remove sites with two or more missing ratios in their time series and containing at least one SILAC ratio higher than 2 or lower than 0.5 (as described in the methods of Francavilla *et al.* [21]). Missing data were imputed with random draws

126 from a truncated distribution, as previously described [25], using the *impute.QRLIC* function from
127 the *imputeLCMD* R package.

128 Data from the Ruprecht *et al.* [22] study were taken from the Supplementary Data file named
129 'Filtered and normalized phosphoproteome dataset'. The raw mass-spectrometry data had been
130 processed using MaxQuant, filtered to include only identified phosphorylated sites with a locali-
131 zation probability of greater than 0.75, and normalized. Sites that did not show a significant change
132 (FDR <1%) either between the untreated parental and lapatinib-treated resistant (SILAC ratios
133 H/L) or between the lapatinib treated parental and lapatinib-treated resistant conditions (SILAC
134 ratios H/M) experimental conditions were filtered from the data, as described in the methods of
135 Ruprecht *et al.* [22]. Missing data were imputed with the same method used for the Francavilla *et*
136 *al.* dataset.

137 Data from the Santra *et al.* study [23] were taken from Supplemental table S2. The raw mass-
138 spectrometry data had been processed using MaxQuant, filtered to include only identified phos-
139 phorylated sites with a localization probability of greater than 0.75; significant sites were identi-
140 fied using a two-sample t-test with FDR. The downloaded dataset was normalized using the *limma*
141 R package function *normalizeBetweenArrays* using the quantile method [26]. Missing data were
142 imputed with the same method used for the Francavilla *et al.* dataset. The data were then filtered
143 to exclude sites that had not been identified by significant in the original analysis by Santra *et al.*

144 Before applying the algorithm, all datasets were clustered based on what was reported in the
145 original publication, where available. The model dataset was clustered using the Fuzzy C-Means
146 (FCM) method [27], with the number of clusters selected based on the temporal trends we could
147 visually identify in the data; generally, silhouette analysis is recommended for selecting the num-
148 ber of clusters using FCM for real experimental datasets [28]. The sites extracted from PSP were

clustered based on what process they were annotated to (as indicated in the "ON_PROCESS" column in the Regulatory_sites file available for download on the PSP website). The regulated phosphorylated sites from Francavilla et al. were clustered using FCM (Figure 3); since the original publication used a cluster number of 6, the same was done here for better comparison. The regulated phosphorylated sites from Ruprecht et al. and Santra et al. were both clustered using the k-means method, with the cluster number selected using the elbow method (Figure S4 and S5, respectively) [29].

Construction of Multilayer Network

Phosphorylation Site – Phosphorylation Site Subnetwork

Edges were drawn between sites in the same cluster that had a Pearson correlation (R2) between all the data points greater than or equal to 0.99 (Figure 1).

Protein - Protein Subnetwork

The protein-protein interaction network was extracted from STRING [30]. All interactors of the proteins included in the phosphoproteomics datasets with an experimental confidence score of greater than 0.4 were included (Figure 1).

Function – Function Subnetwork

We used either GOBP terms or KEGG pathways as functional annotators in this work. If GOBP terms were included in the multilayer network, the *GOSemSim* package from Bioconductor [31] was used to calculate the semantic similarity of enriched GOBP terms. An edge was drawn between terms with semantic similarity greater than 0.7, as calculated using the Wang method included in the *goSim* function of *GOSemSim* [31,32]. In the case of KEGG pathways, edges were drawn between pathways that had greater than 70% pairwise similarity in their functional annotation profiles, following the method described in Stoney *et al.* [33] (Figure 1).

Phosphorylation Site – Protein Bipartite Edges

Sites and proteins had an edge between them if the residue was found on that protein. Therefore, sites will only have one edge, but proteins will have edges to all the sites found on that protein that were differentially regulated in the data set (Figure 1).

Protein – Function Bipartite Edge

We assumed that closely connected nodes in the protein-protein subnetwork would more likely be involved in similar biological processes. Therefore, we computed modules of the protein-protein subnetwork using the Louvain module-detection method [34]. Proteins from each module were analyzed for enrichment (hypergeometric test with Benjamini-Hochberg correction, FDR < 0.05%) of functional annotations (from either the "GO_Biological_Process_2018" or "KEGG_2019_Human" libraries, included in enrichR and listed on the EnrichR website) using the *enrichR* [35] R interface. This increased the specificity of terms to be included in the network. When GO terms were included, high frequency (annotated to more than 5% of genes) and semantically redundant terms (similarity > 0.9) were filtered using the Bioconductor *GOSemSim* [31] and *GO.db* packages [36] (Figure 1).

Random Walk on Heterogeneous Network

The heterogeneous network can be represented as an adjacency matrix as follows:

$$A = \begin{bmatrix} A_{RR} & A_{RP} & 0 \\ A_{PR} & A_{PP} & A_{PF} \\ 0 & A_{FP} & A_{FF} \end{bmatrix} \quad (1)$$

where: A_{RR} are site-site associations, A_{PP} are protein-protein associations, A_{FF} are function-function associations, A_{RP} are site-protein associations with A_{PR} as the transpose and A_{PF} are protein-function associations with A_{FP} as the transpose.

As described in previous work [15], a transition matrix (M) was calculated for use in the first stage of the algorithm:

$$M = \begin{bmatrix} M_{RR} & M_{RP} & 0 \\ M_{RP^T} & M_{PP} & M_{PF} \\ 0 & M_{PF^T} & M_{FF} \end{bmatrix} \tag{2}$$

The bipartite inter-subgraph transition matrices (M_{RP} and M_{PF}) were calculated as:

$$(M_{RP})_{i,j} = \begin{cases} \lambda\,(A_{RP})_{i,j} \Big/ \sum_j (A_{RP})_{i,j}, if \sum_j (A_{RP})_{i,j} \neq 0 \\ 0, otherwise \end{cases} \tag{3}$$

$$(M_{PF})_{i,j} = \begin{cases} \lambda\,(A_{PF})_{i,j} \Big/ \sum_j (A_{PF})_{i,j}, if \sum_j (A_{PF})_{i,j} \neq 0 \\ 0, otherwise \end{cases} \tag{4}$$

where λ is the transition probability (i.e., the likelihood of the walker moving between two layers of the network).

The intra-subgraph transition matrices (M_{RR}, M_{PP} and M_{FF}) were calculated as:

$$(M_{RR})_{i,j} = \begin{cases} (A_{RR})_{i,j} \Big/ \sum_j (A_{RR})_{i,j}, if \sum_j (A_{RP})_{i,j} = 0 \\ (1-\lambda)\,(A_{RR})_{i,j} \Big/ \sum_j (A_{RR})_{i,j}, otherwise \end{cases} \tag{5}$$

$$(M_{PP})_{i,j} = \begin{cases} (A_{PP})_{i,j} \Big/ \sum_j (A_{PP})_{i,j}, if \sum_j (A_{PR})_{i,j}, (A_{PF})_{i,j} = 0 \\ (1-\lambda)\,(A_{PP})_{i,j} \Big/ \sum_j (A_{PP})_{i,j}, otherwise \end{cases} \tag{6}$$

$$(M_{FF})_{i,j} = \begin{cases} (A_{FF})_{i,j} \Big/ \sum_j (A_{FF})_{i,j}, if \sum_j (A_{FP})_{i,j} = 0 \\ (1-\lambda)\,(A_{FF})_{i,j} \Big/ \sum_j (A_{FF})_{i,j}, otherwise \end{cases} \tag{7}$$

RWHN is a ranking algorithm; nodes are ranked based on the probabilities of finding the random walker at a given node in the steady state, having started at a given seed node or set of seed nodes. In this work we set the seed nodes to be those sites belonging to a particular cluster. The probability of finding the random walker at each node for each step is calculated based on the iterative equation:

$$\begin{cases} P_{s+1} = (1-r) \times M^T \times P_s + r \times P_0 \\ P_{s+1} - P_s \leq 10^{-6} \end{cases} \quad (8)$$

203 where r is the restart probability (set to 0.7 as described in Kohler *et al.* [37]), P_0 is the initial
204 probability vector and P_s is the probability vector at step s. P0 was calculated such that all seed
205 nodes were given equal probabilities with their sum equal to 1. All other nodes in the site-site
206 subnetwork were assigned an initial probability of 0. Nodes in other subnetworks were assigned
207 equal probabilities with their sum equal to 1 and weighted with the tunable parameters ηP and ηF,
208 that are used to weight the influence of each layer.

209 The output of the algorithm is a ranked list of all the nodes, based on the probability of finding
210 the random walker at each node in the steady state. This list is filtered by retaining functional
211 annotations and removing proteins and sites. We remove annotations that are ranked in the same
212 position regardless of seed node, in order to focus on specific functions related to each cluster.
213 The top 5% of functions in the probability distribution are retained.

214 We implemented the algorithm in R using packages available from Bioconductor and CRAN.
215 The source code is available at www.github.com/jowatson2011/RWHN_phosphoproteomics and
216 an R package for general use of the tool can be found at github.com/JoWatson2011/phosphoR-
217 WHN. RWHN on the validation network took less than 30 seconds to run however the larger
218 experimental data sets took several hours on a moderately powerful computer (32GB RAM, Intel
219 i7-4770 Processor).

220 **Overrepresentation Analysis (ORA)**

221 The names of modified proteins in each cluster were used as input for the *enrichR* R interface
222 [35]. The libraries "GO_Biological_Process_2018" or "KEGG_2019_Human" (included in enrichR
223 and listed on the EnrichR website) were used depending on which was used for the RWHN

224 analysis of the same data. The list of overrepresented terms was filtered to only include those with
225 an FDR < 0.05.

226 ## 4. Results

227 ### Overview of Algorithm

228 To associate phosphorylated sites of unknown function to potential cellular functions we devel-
229 oped an algorithm to apply to shotgun phosphoproteomics data. First, in order to help experimental
230 biologists to identify the context- or perturbation-specific roles of modified proteins changing in
231 each given experiment, a multilayer heterogeneous network is constructed based on the regulation
232 of phosphorylated sites. Regulated phosphorylated sites may be defined differently by the user
233 depending on the quantitation method used in their phosphoproteomics experiment (e.g., label-
234 free quantification, SILAC) or their experimental question. The network represents three layers
235 of biological entities and information: regulated phosphorylated sites, protein-protein interaction,
236 and biological function (Figure 1). We then apply a ranking algorithm, RWHN, which ranks nodes
237 of each layer based on: (i) distance from the phosphorylated sites of interest, which are assigned
238 as 'seed' nodes and (ii) the topology of the multilayer heterogeneous network [15]. Functions that
239 are highly ranked can be considered more correlated with a set of seed nodes.

240 In the multilayer heterogeneous network, edges are drawn between sites based on similarity in
241 the regulatory pattern of their phosphorylation which we determine using k-means or fuzzy C-
242 means clustering. For the protein layer, a PPI network is constructed of the phosphorylated pro-
243 teins and their interactors using the STRING database [30]. Interactors are included to account for
244 non-phosphorylated proteins, or those below the limit of detection of the experiment [38]. To get a
245 comprehensive and specific list of functional annotations, we identified closely connected groups
246 of proteins in the PPI network using module detection and performed functional enrichment

247 analysis on these modules. Edges between functional annotations are drawn based on functional
248 similarity and overlap [31,33].

249 The RWHN algorithm simulates a walker moving from a starting node(s) (called a seed) and
250 then node to node through the multilayer network. Each step is influenced by the probability of
251 transition to another layer (λ), the weighting of the protein and function layers (η_P and η_F) and the
252 probability of restart (that is, teleportation back to the seed node(s), *r*). The output of RWHN
253 consists in a list of ranks for all the nodes in the network based on the likelihood of the walker
254 reaching that node.

255 To optimize the algorithm, we ran RWHN with each of these parameters (λ, r, η_P and η_F) tested
256 over a range of values (0.1 – 0.9), changing one whilst setting all others to 0.5 (Figure S1A).
257 Performance was decidedly stable over the range of η_P and η_F however altering λ and *r* resulted
258 in differential ranking depending on the parameter value. Previous work has suggested an ideal λ
259 and *r* of 0.7 [15,37,39], whilst η_P and η_F were set to 0.7 and 0.3 respectively to prioritize movement in
260 the protein layer and reduce the number of terms having the same rank regardless of seed.

261 The parameters used in the construction of the PPI network were also assessed. Proteins inter-
262 acting with the phosphorylated proteins found in a given sample were extracted from STRING;
263 those proteins whose interaction had a STRING experimental confidence score above a given
264 threshold were included in the multilayer heterogeneous network. To investigate the impact of
265 choosing different STRING confidence scores on the results, we tested a confidence score range
266 of 0.1 – 0.9. First, we looked at whether connectivity of the graph was altered by the score. As
267 expected, the greater the confidence score, the more components the PPI were split into; above a
268 score of 0.7, the PPI had two or more components (Figure S1B). We next investigated whether
269 the RWHN results were affected by changing the STRING confidence score increasing

270 components within the protein layer. Using weighted-tau correlation[40] to compare the rankings
271 from each set of results, we found that the correlation was generally in the range of 0.8 – 1.0, with
272 the lowest value being 0.54 between networks constructed with 0.1 or 0.9 confidence threshold,
273 which were the extremes of the range tested.

274 **Validation 1: Model of MAPK/ERK pathway**

275 MAPK/ERK signalling has been well studied and the temporal phosphorylation status of com-
276 ponent proteins in response to growth factor stimulus are relatively established [41,42](Figure 2A).
277 Based on this general understanding, we compiled a simple validation dataset of phosphorylation
278 dynamics at particular sites of the main signalling proteins within the pathway (Figure 2B). Sites
279 were chosen based on whether their phosphorylation is known to activate or inactivate protein
280 activity, as recorded in the PSP database [6]. We clustered the data into 5 clusters, referred to here
281 as clusters 1-5, using the fuzzy c-means algorithm (Figure 2B). The features of the multilayer
282 network that was constructed are summarized in Table 1. Enrichment of GOBP terms was used
283 to form the functional annotation layer of the network.

284 We ran the RWHN algorithm over the multilayer heterogeneous network with seed nodes set to
285 all the sites belonging to one of the clusters; this was then repeated for each cluster (Figure 2C).
286 The highest ranked GOBP term was the same ("protein autophosphorylation") regardless of the
287 seed nodes. However, it was possible to differentiate between the five clusters based on the rank-
288 ing of terms below the first one.

289

290 Table 1. Multilayer heterogeneous network, constructed from MAPK/ERK validation data. GOBP
291 terms were included as functional annotations.

Subnetwork	Edges	Nodes

Site-site	28	19
Protein-protein	932	313
Function-function	148	88
Site-protein	19	19 sites, 8 proteins
Protein-function	1796	261 proteins, 298 functions

292

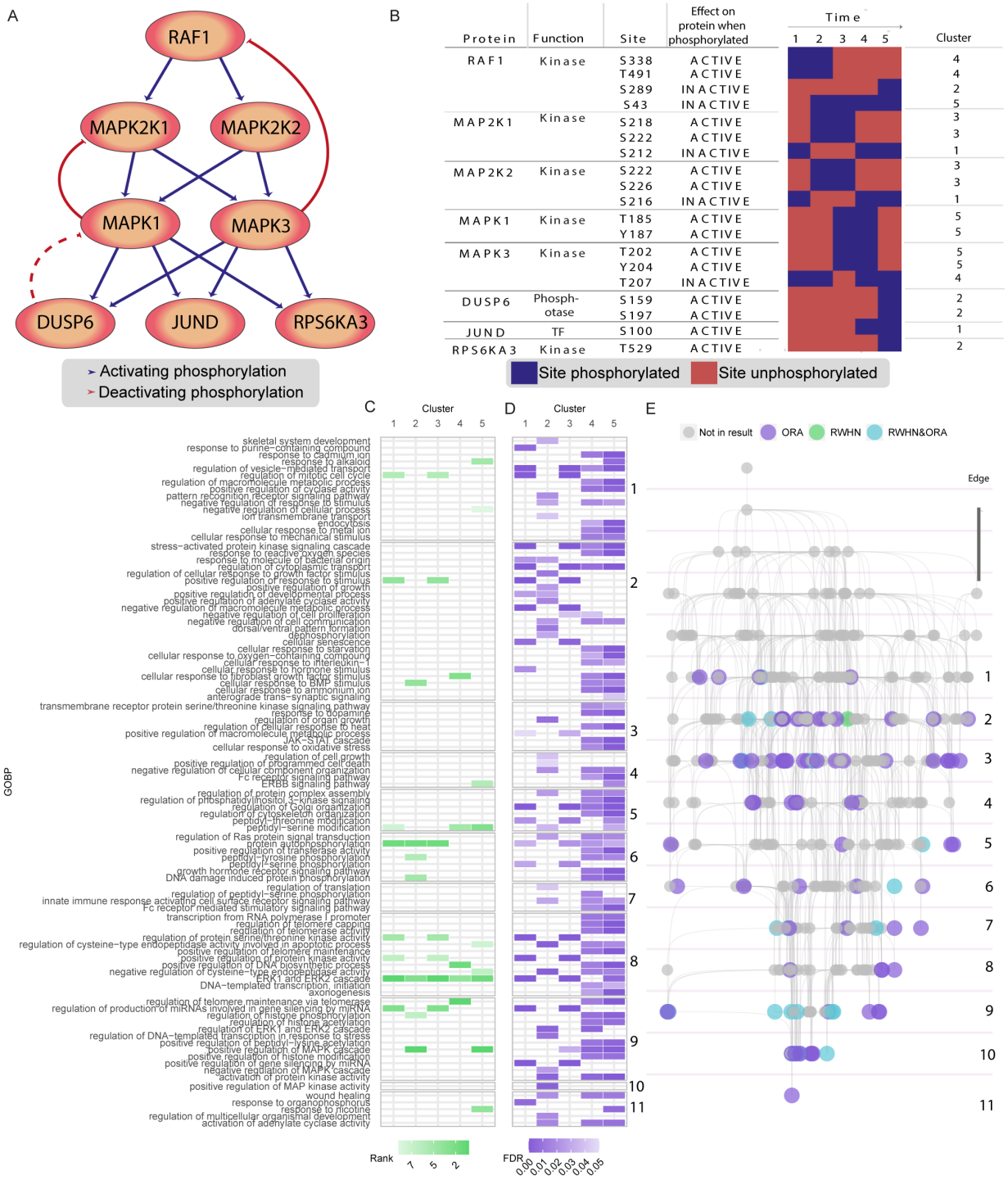

Figure 2. Site- and gene-centric analysis of validation data. A) Construction of validation data was based on a traditional representation of the MAPK/ERK pathway. B) A validation dataset was constructed based on the MAPK/ERK pathway, simulating phosphorylation dynamics over

297 time after pathway activation. The sites were clustered using fuzzy c-means clusters. These data
298 were used to construct a heterogeneous multilayer network. C) RWHN results with sites annotated
299 to functional roles in PSP; seed nodes are equivalent to the clusters. D) ORA results with modified
300 proteins contained in toy data. E) GO hierarchy, which has been subset to include only the parents
301 of terms that occurred in either the RHWN or ORA analysis. Terms that occur in either set of
302 results are colored in purple or green, respectively, with terms that occur in both colored in light
303 blue.

304 Where available, we could use the biological process annotations in PSP (v6.5.9.3) as a 'bench-
305 mark' for the highly ranked terms associated to each cluster. RPS6KA3_Y529, annotated to
306 "apoptosis, altered" in PSP is found in cluster 2, along with DUSP6 sites; this cluster highly ranks
307 "positive regulation of programmed cell death". Of the four RAF1 sites included in this model
308 dataset, two were annotated to "cell cycle regulation" in PSP: RAF1_S289, in cluster 2, and
309 RAF1_S338, in cluster 5. These two clusters both rank "regulation of mitotic cell cycle" in the
310 top 5% of terms.

311 Largely due to the inherent step in our method in which the redundant terms are reduced in the
312 multilayer heterogeneous network, fewer terms were found in the results of RWHN than ORA.
313 We next wanted to assess whether the terms in the RWHN result were drawn from a particular
314 level of the GO hierarchy; if they were, this would suggest a bias towards more specific or more
315 broad terms compared to ORA. From the GO hierarchy, we extracted the parent and ancestor
316 terms of the terms found in each set of the results (Figure 2E). We found that RWHN terms were
317 drawn from the same range of the hierarchy as the ORA terms, with slightly more coming from
318 lower in the hierarchy, indicating the results have more specificity than the ORA results. We note
319 that there is also less redundancy in the RWHN results, despite the ORA results also being reduced

320 for semantically similar / redundant terms. For example, the terms "regulation of ERK1 and ERK2
321 cascade" and "ERK1 and ERK2 cascade" both come up in the ORA results and are associated to
322 different clusters.

323 To assess the robustness of the algorithm, we performed a random permutation control. RWHN
324 was run one hundred times with the seeds set as before, random permutations of the subnetworks
325 and bipartite edges maintained. Kernel Density Estimation (KDE) was calculated to assess how
326 often each GO term occurred at each rank in the 100 random permutations for each set of seed
327 nodes. In each case, there were a subset of terms that were more likely to have a rank greater than
328 50, however none strongly correlated with the actual rankings for each set of seed nodes (Figure
329 S2A). This confirms that the rankings are not random, but primarily determined by the network
330 topology. We next investigated the rate of potential false positives in the results. Previous imple-
331 mentations of RWHN, primarily using genomics data, have utilized an arbitrary threshold of the
332 top *x* ranked terms, or the top *x*% of ranked terms (based on the probability vector as calculated
333 in equation 8). A threshold that is too stringent would not remove lower-ranking terms from the
334 results, whilst a too-low threshold would increase the amount of noise in the data. Using the results
335 of RWHN run on the randomly permuted networks we calculated the probability that the "true"
336 ranking (i.e. from RWHN run on the non-permuted network) was different from the random rank-
337 ings ($p < 0.05$, Mann-Whitney U test with Benjamini-Hochberg adjustment [43,44]). We found that
338 most of the rankings differed from random (Figure S2B). The terms that had $p > 0.05$ were
339 checked against the RWHN results with different thresholds selected (top 1%, 5%, 10% and 15%
340 of ranked terms); none were found above the 1% thresholds for any of the clusters, and only one
341 term ("peptidyl-serine modification" in cluster 2) was found above the 5% and 10% thresholds

342 (Figure S2B). We chose to set the default threshold to the top 5% of terms to be more conservative
343 whilst retaining useful annotations.
344 For a given set of seed nodes, the algorithm is capable of giving high ranks to functions with
345 known associations to those sites. It is also capable of predicting non-random, reasonable func-
346 tions for sites of unknown function in this context.

347 **Validation 2: Classification of PhosphoSitePlus annotated sites**

348 A comprehensive benchmark of dynamically regulated phosphorylated sites is not currently
349 available, due to the lack of phosphorylated sites with a regulatory pattern universally defined
350 independent of the experimental conditions. Therefore, we used the static classifications of phos-
351 phorylated site function recorded in PSP to benchmark the predictive power of our algorithm. The
352 PSP database has annotations to biological processes for ~4000 human phosphorylated sites. As
353 these annotations are non-standard, each one was mapped to the most closely related GOBP term,
354 where available (Table S1). The majority of sites were annotated to signal transduction, gene ex-
355 pression or cell differentiation (Figure 3A). Of these, 1496 sites were annotated to more than one
356 function; as these annotations are manually assigned based on literature searches, the multiple
357 functions may be due to the differences in experimental questions in the source datasets. The sites
358 were clustered based on which function they were annotated to and analyzed with RWHN and
359 ORA. The GOBP terms in the results of both methods were associated to the child terms of each
360 mapped PSP GO term, per the GO hierarchy. The terms in the results of both methods showed a
361 similar distribution to the terms in PSP as a whole, the main exception being in the cell differen-
362 tiation category (Figure 3B). The two methods showed a considerable difference in the number of
363 terms in the output, with ORA resulting in several hundred more terms in the output than RWHN.
364 To test whether the two sets of results were drawn from the same parts of the GO hierarchy (with

365 those from the top of the hierarchy being broader and those at the bottom being more specific),
366 we constructed a tree based on the GO hierarchy. The tree was then divided into levels, as in
367 Figure 2E, to capture terms that were of similar descriptiveness. Finally, we counted the number
368 of terms that came up in the RWHN or ORA results (Figure 3C). Both sets of results draw from
369 the same part of the hierarchy, with a skew towards the broader terms. We therefore concluded
370 that RWHN resulted in as descriptive but more restricted and focused annotations than ORA. This
371 was notable given that RWHN did not associate any terms to the smaller categories in PSP, such
372 as exocytosis, endocytosis, cell growth and autophagy (Figure 3B).
373

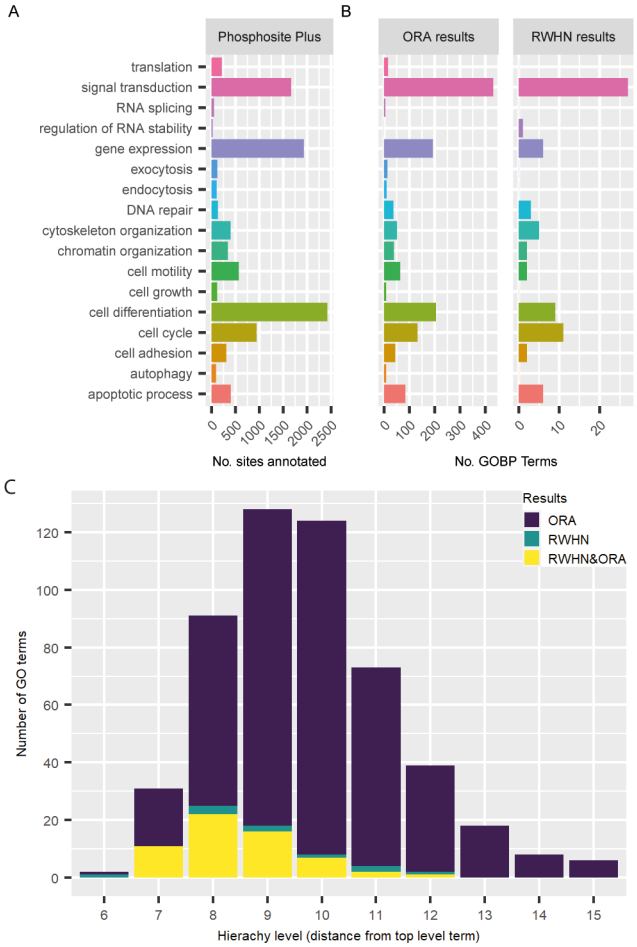

Figure 3. Distribution of annotations and classifications of sites extracted from PhosphoSitePlus. A) Distributions of functionally annotated sites (to mapped GO term). B) Distribution of terms in ORA results and RWHN results when analyzing functionally annotated sites from PSP. C) Number of terms from ORA or RWHN that are from different levels of the GO hierarchy

374

375

376 **Experimental Case Study 1: Dissecting EGF- and TGF-α-Induced Dynamic Phosphory-**
377 **lation**

378 Given that PSP contains static annotations of sites from various sources, we wanted to test our
379 algorithm on experimental datasets with controlled perturbations. We reasoned that this would
380 allow us to assess whether our algorithm could differentially associate sites to their context-de-
381 pendent function. The phosphoproteomics data retrieved from Francavilla *et al.* [21] describes the
382 effect in HeLa cells of stimulation with EGF or TGF-α over a period of 90 minutes (with time
383 points at 1, 8, 40 and 90 minutes). In this study, one of the findings was that EGF or TGF-α
384 stimulation of EGFR induce receptor degradation or recycling, respectively. TGF-α was associ-
385 ated with a more potent mitogenic and migratory response than EGF over time [21]. Further details
386 on the experimental design and results from the publication can be found in Supplementary Table
387 S2. Phosphorylated sites from Supplementary Table S1 of the original publication were filtered
388 based on regulation by EGF or by TGF-α and divided based on which stimuli the regulation was
389 dependent on. The separated data were clustered into 6 clusters using the fuzzy C-means method,
390 as per the original publication, with each cluster representing a distinct dynamic profile of phos-
391 phorylation (Figure S3). A multilayer heterogeneous network was constructed for both sets of
392 data, described in Table 2 and Table 3, respectively.

393

394 Table 2. Multilayer heterogeneous network, constructed from Francavilla *et al.* [21] EGF-regulated

395 phosphorylated sites. GOBP terms were included as functional annotations.

Subnetwork	Edges	Nodes
Site-site	4347	733
Protein-protein	16654	4072
Function-function	532	544
Site-protein	733	733 sites, 433 proteins
Protein-function	1223	115 proteins, 532 functions

396

397

398 Table 3. Multilayer heterogeneous network, constructed from Francavilla *et al.* [21] TGFα-regulated

399 phosphorylated sites. GOBP terms were included as functional annotations.

Subnetwork	Edges	Nodes
Site-site	3085	675
Protein-protein	16556	3960
Function-function	332	496
Site-protein	675	675 sites, 403 proteins
Protein-function	1015	109 proteins, 486 functions

400

401 Several biologically relevant terms were differentially ranked in the EGF and TGF-α networks

402 (Figure 4A,C). Consistent with the original publication, the term "regulation of ERK1 and ERK2

403 cascade" was highly ranked using RWHN when seeds were set to sites in cluster 2 (representing

404 EGF late responders) for the EGF network and in cluster 1 (representing TGF-α early responders)

405 for the TGF-α network. Despite their central role to TGF-α signalling, when we performed

406 standard ORA enrichment terms relating to MAPK/ERK were not found in any of the clusters
407 (Figure 4D). However, both ORA and our method highlighted the role of the proteins belonging
408 to TGF-α cluster 1 in regulating EGFR/ERBB signaling, with terms referring to regulation of
409 these pathways ranked highly (Figure 4C,D). We used cluster 2 in the EGF condition and cluster
410 1 in the TGF-α condition to verify the robustness and accuracy of our approach. As the
411 MAPK/ERK cascade is well studied in respect to EGF/TGF-α signaling, many of its associated
412 sites have documented functions that we could use to benchmark our results. EGF cluster 2 con-
413 tains sites of several known players of the MAPK/ERK cascades, including RSP6KA3_S375,
414 SOS1 (T1119, S1137), RAF1 (S289, S96, S301), JUN_S243 and JUNB_259. All of these sites
415 are predicted MAPK1/MAPK3 targets, with the exception of SOS1_T1119, which is a MAP2K1
416 target [7]. As this cluster represents those sites phosphorylated late in the time course, we would
417 expect ERK1/2 feedback regulation to emerge. Besides confirming the term "regulation of ERK1
418 and ERK2 cascade" in EGF cluster 2, results from the RHWN algorithm add detail to this picture,
419 with "establishment of protein localization to organelle" ranked highly in this cluster (Figure 4A).
420 This finding confirms the conclusion of Francavilla *et al*. of EGFR trafficking to the lysosome,
421 and subsequent degradation, when stimulated by EGF [21]. EGF cluster 2 is the only one which did
422 not highly rank "regulation of clathrin-dependent endocytosis" compared to the 5 other clusters;
423 as this cluster represents sites that are highly phosphorylated late in the time-course, this coincides
424 with the understanding of receptor endocytosis as a process regulated in the early stage. This clus-
425 ter is one of the five that highly ranks "regulation of cell migration" (Figure 4A); PSP also anno-
426 tates several of the sites in this cluster to cell motility (PTPN12_S571, SLC9A1_S703,
427 FLNA_S2152).
428

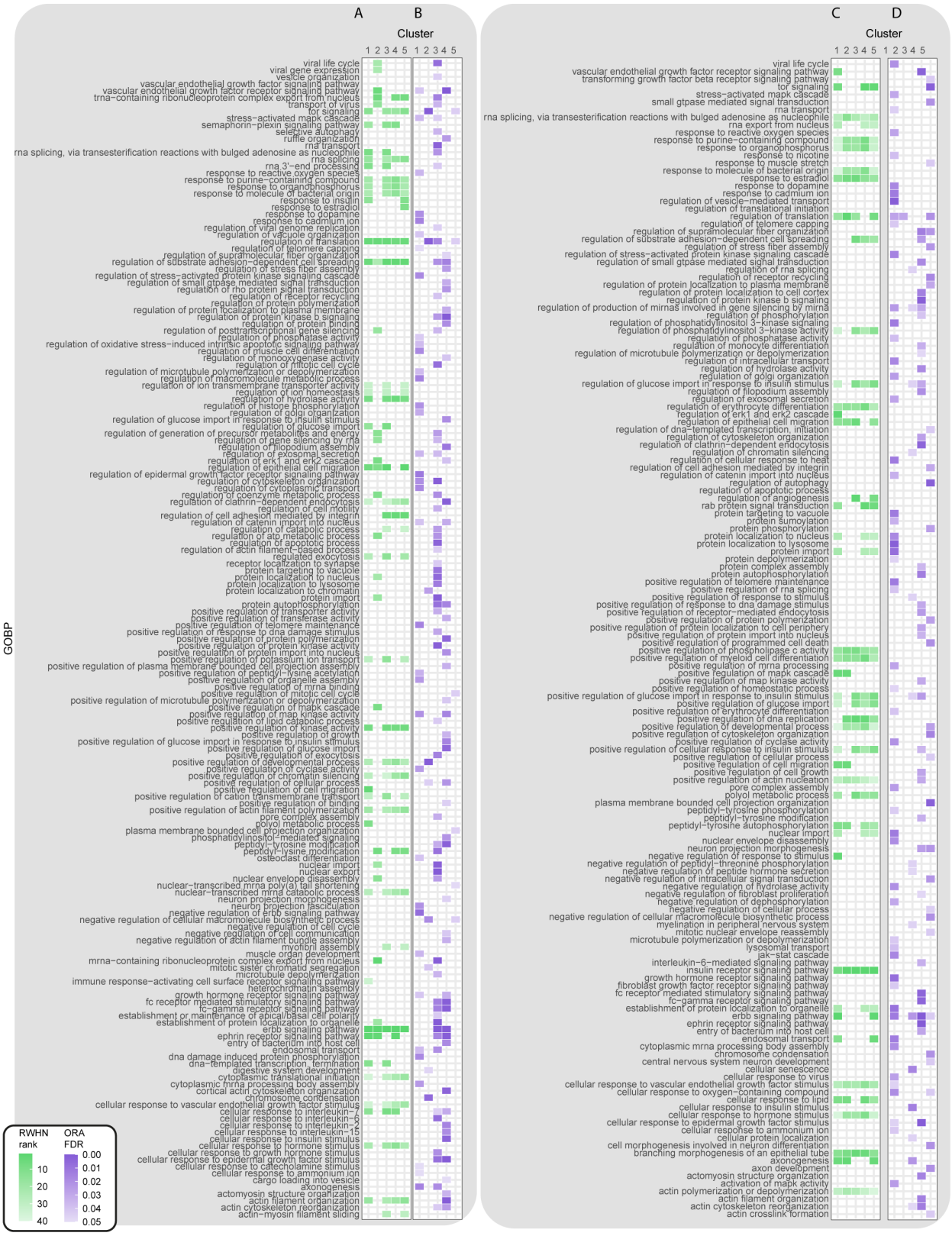
A
B
C
D
Cluster
1 2 3 4 5
GOBP
viral life cycle
viral gene expression
vesicle organization
vascular endothelial growth factor signaling pathway
vascular endothelial growth factor receptor signaling pathway
trna-containing ribonucleoprotein complex export from nucleus
transport of virus
tor signaling
stress-activated mapk cascade
semaphorin-plexin signaling pathway
selective autophagy
ruffle organization
rna transport
rna splicing, via transesterification reactions with bulged adenosine as nucleophile
rna splicing
rna 3'-end processing
response to reactive oxygen species
response to purine-containing compound
response to organophosphorus
response to molecule of bacterial origin
response to insulin
response to estradiol
response to dopamine
response to cadmium ion
regulation of viral genome replication
regulation of vacuole organization
regulation of translation
regulation of telomere capping
regulation of supramolecular fiber organization
regulation of substrate adhesion-dependent cell spreading
regulation of stress fiber assembly
regulation of stress-activated protein kinase signaling cascade
regulation of small gtpase mediated signal transduction
regulation of rho protein signal transduction
regulation of receptor recycling
regulation of protein polymerization
regulation of protein localization to plasma membrane
regulation of protein kinase b signaling
regulation of protein binding
regulation of posttranscriptional gene silencing
regulation of phosphatase activity
regulation of oxidative stress-induced intrinsic apoptotic signaling pathway
regulation of muscle cell differentiation
regulation of monooxygenase activity
regulation of mitotic cell cycle
regulation of microtubule polymerization or depolymerization
regulation of macromolecule metabolic process
regulation of ion transmembrane transporter activity
regulation of ion homeostasis
regulation of hydrolase activity
regulation of histone phosphorylation
regulation of golgi organization
regulation of glucose import in response to insulin stimulus
regulation of glucose import
regulation of generation of precursor metabolites and energy
regulation of gene silencing by rna
regulation of filopodium assembly
regulation of exosomal secretion
regulation of erk1 and erk2 cascade
regulation of epithelial cell migration
regulation of epidermal growth factor receptor signaling pathway
regulation of cytoskeleton organization
regulation of cytoplasmic transport
regulation of coenzyme metabolic process
regulation of clathrin-dependent endocytosis
regulation of cell motility
regulation of cell adhesion mediated by integrin
regulation of catenin import into nucleus
regulation of catabolic process
regulation of atp metabolic process
regulation of apoptotic process
regulation of actin filament-based process
regulated exocytosis
receptor localization to synapse
protein targeting to vacuole
protein localization to nucleus
protein localization to lysosome
protein localization to chromatin
protein import
protein autophosphorylation
positive regulation of transporter activity
positive regulation of transferase activity
positive regulation of telomere maintenance
positive regulation of response to dna damage stimulus
positive regulation of protein polymerization
positive regulation of protein kinase activity
positive regulation of protein import into nucleus
positive regulation of potassium ion transport
positive regulation of plasma membrane bounded cell projection assembly
positive regulation of peptidyl-lysine acetylation
positive regulation of organelle assembly
positive regulation of mrna binding
positive regulation of mitotic cell cycle
positive regulation of microtubule polymerization or depolymerization
positive regulation of mapk cascade
positive regulation of map kinase activity
positive regulation of lipid catabolic process
positive regulation of kinase activity
positive regulation of growth
positive regulation of glucose import in response to insulin stimulus
positive regulation of glucose import
positive regulation of exocytosis
positive regulation of developmental process
positive regulation of cyclase activity
positive regulation of chromatin silencing
positive regulation of cellular process
positive regulation of cell migration
positive regulation of cation transmembrane transport
positive regulation of binding
positive regulation of actin filament polymerization
pore complex assembly
polyol metabolic process
plasma membrane bounded cell projection organization
phosphatidylinositol-mediated signaling
peptidyl-tyrosine modification
peptidyl-lysine modification
osteoclast differentiation
nuclear import
nuclear export
nuclear envelope disassembly
nuclear-transcribed mrna poly(a) tail shortening
nuclear-transcribed mrna catabolic process
neuron projection morphogenesis
neuron projection fasciculation
negative regulation of erbb signaling pathway
negative regulation of cellular macromolecule biosynthetic process
negative regulation of cell cycle
negative regulation of cell communication
negative regulation of actin filament bundle assembly
myofibril assembly
muscle organ development
mrna-containing ribonucleoprotein complex export from nucleus
mitotic sister chromatid segregation
microtubule depolymerization
immune response-activating cell surface receptor signaling pathway
heterochromatin assembly
growth hormone receptor signaling pathway
fc receptor mediated stimulatory signaling pathway
fc-gamma receptor signaling pathway
establishment or maintenance of apical/basal cell polarity
establishment of protein localization to organelle
erbb signaling pathway
ephrin receptor signaling pathway
entry of bacterium into host cell
endosomal transport
dna damage induced protein phosphorylation
dna-templated transcription, termination
digestive system development
cytoplasmic translational initiation
cytoplasmic mrna processing body assembly
cortical actin cytoskeleton organization
chromosome condensation
cellular response to vascular endothelial growth factor stimulus
cellular response to interleukin-7
cellular response to interleukin-6
cellular response to interleukin-2
cellular response to interleukin-15
cellular response to insulin stimulus
cellular response to hormone stimulus
cellular response to growth hormone stimulus
cellular response to epidermal growth factor stimulus
cellular response to catecholamine stimulus
cellular response to ammonium ion
cargo loading into vesicle
axonogenesis
actomyosin structure organization
actin filament organization
actin cytoskeleton reorganization
actin-myosin filament sliding
RWHN rank
10
20
30
40
ORA FDR
0.00
0.01
0.02
0.03
0.04
0.05
viral life cycle
vascular endothelial growth factor receptor signaling pathway
transforming growth factor beta receptor signaling pathway
tor signaling
stress-activated mapk cascade
small gtpase mediated signal transduction
rna transport
rna splicing, via transesterification reactions with bulged adenosine as nucleophile
rna export from nucleus
response to reactive oxygen species
response to purine-containing compound
response to organophosphorus
response to nicotine
response to muscle stretch
response to molecule of bacterial origin
response to estradiol
response to dopamine
response to cadmium ion
regulation of vesicle-mediated transport
regulation of translational initiation
regulation of translation
regulation of telomere capping
regulation of supramolecular fiber organization
regulation of substrate adhesion-dependent cell spreading
regulation of stress fiber assembly
regulation of stress-activated protein kinase signaling cascade
regulation of small gtpase mediated signal transduction
regulation of rna splicing
regulation of receptor recycling
regulation of protein localization to plasma membrane
regulation of protein localization to cell cortex
regulation of protein kinase b signaling
regulation of production of mirnas involved in gene silencing by mirna
regulation of phosphorylation
regulation of phosphatidylinositol 3-kinase signaling
regulation of phosphatidylinositol 3-kinase activity
regulation of phosphatase activity
regulation of monocyte differentiation
regulation of microtubule polymerization or depolymerization
regulation of intracellular transport
regulation of hydrolase activity
regulation of golgi organization
regulation of glucose import in response to insulin stimulus
regulation of filopodium assembly
regulation of exosomal secretion
regulation of erythrocyte differentiation
regulation of erk1 and erk2 cascade
regulation of epithelial cell migration
regulation of dna-templated transcription, initiation
regulation of cytoskeleton organization
regulation of clathrin-dependent endocytosis
regulation of chromatin silencing
regulation of cellular response to heat
regulation of cell adhesion mediated by integrin
regulation of catenin import into nucleus
regulation of autophagy
regulation of apoptotic process
regulation of angiogenesis
rab protein signal transduction
protein targeting to vacuole
protein sumoylation
protein phosphorylation
protein localization to nucleus
protein localization to lysosome
protein import
protein depolymerization
protein complex assembly
protein autophosphorylation
positive regulation of telomere maintenance
positive regulation of rna splicing
positive regulation of response to stimulus
positive regulation of response to dna damage stimulus
positive regulation of receptor-mediated endocytosis
positive regulation of protein polymerization
positive regulation of protein localization to cell periphery
positive regulation of protein import into nucleus
positive regulation of programmed cell death
positive regulation of phospholipase c activity
positive regulation of myeloid cell differentiation
positive regulation of mrna processing
positive regulation of mapk cascade
positive regulation of map kinase activity
positive regulation of homeostatic process
positive regulation of glucose import in response to insulin stimulus
positive regulation of glucose import
positive regulation of erythrocyte differentiation
positive regulation of dna replication
positive regulation of developmental process
positive regulation of cytoskeleton organization
positive regulation of cyclase activity
positive regulation of cellular response to insulin stimulus
positive regulation of cellular process
positive regulation of cell migration
positive regulation of cell growth
positive regulation of actin nucleation
pore complex assembly
polyol metabolic process
plasma membrane bounded cell projection organization
peptidyl-tyrosine phosphorylation
peptidyl-tyrosine modification
peptidyl-tyrosine autophosphorylation
nuclear import
nuclear envelope disassembly
neuron projection morphogenesis
negative regulation of response to stimulus
negative regulation of peptidyl-threonine phosphorylation
negative regulation of peptide hormone secretion
negative regulation of intracellular signal transduction
negative regulation of hydrolase activity
negative regulation of fibroblast proliferation
negative regulation of dephosphorylation
negative regulation of cellular process
negative regulation of cellular macromolecule biosynthetic process
myelination in peripheral nervous system
mitotic nuclear envelope reassembly
microtubule polymerization or depolymerization
lysosomal transport
jak-stat cascade
interleukin-6-mediated signaling pathway
insulin receptor signaling pathway
growth hormone receptor signaling pathway
fibroblast growth factor receptor signaling pathway
fc receptor mediated stimulatory signaling pathway
fc-gamma receptor signaling pathway
establishment of protein localization to organelle
erbb signaling pathway
ephrin receptor signaling pathway
entry of bacterium into host cell
endosomal transport
cytoplasmic mrna processing body assembly
chromosome condensation
central nervous system neuron development
cellular senescence
cellular response to virus
cellular response to vascular endothelial growth factor stimulus
cellular response to oxygen-containing compound
cellular response to lipid
cellular response to insulin stimulus
cellular response to hormone stimulus
cellular response to epidermal growth factor stimulus
cellular response to ammonium ion
cellular protein localization
cell morphogenesis involved in neuron differentiation
branching morphogenesis of an epithelial tube
axonogenesis
axon development
actomyosin structure organization
activation of mapk activity
actin polymerization or depolymerization
actin filament organization
actin cytoskeleton reorganization
actin crosslink formation

429

430 **Figure 4.** Site-centric and gene-centric analysis of Francavilla *et al.*[21] datasets. (A) RWHN results
431 related to EGF regulated sites. (B) ORA results related to proteins modified upon EGF stimula-
432 tion. (C) RWHN results related to TGF-α regulated sites. (D) ORA results related to proteins
433 modified upon TGF-α stimulation.

434

435 TGF-α cluster 1, on the other hand, contains sites that are phosphorylated within the first eight
436 minutes upon TGF-α stimulation. Accordingly, this cluster contains different members of the
437 MAPK/ERK cascade, such as the canonical activating sites of MAPK1, MAPK3 and MAPK14
438 (also known as p38) and several sites on EGFR (EGFR_S991, EGFR_S995, EGFR_T693).
439 EGFR_S991. A few of these sites, such as EGFR_T693, are annotated to "receptor internaliza-
440 tion" in PSP. This cluster also contains several phosphorylated sites on known players in receptor
441 trafficking, including RAB7A_Y183 and RAB11B_Y8 which are highlighted in the original pub-
442 lication [21], along with CBL_Y674 and SH3BP4_T118. Our algorithm ranked terms such as "en-
443 dosomal transport,", "establishment of protein localization to organelle" and "rab protein signal
444 transduction" high when seed nodes were set to the sites found in this cluster (Figure 4C). This
445 was only partially captured by the ORA (Figure 4D), which showed enrichment of the term "reg-
446 ulation of vesicle mediated transport" but also "protein localization to the lysosome", the opposite
447 of the experimentally derived conclusion of Francavilla *et al*.

448 EGF cluster 1 representing phosphorylated cycling sites ranks both "regulation of cell migra-
449 tion" and "positive regulation of cell migration" in the top 5% of terms but did not have a similar
450 association with trafficking terms as TGF-α cluster 1 in the RWHN output. Consistent with Fran-
451 cavilla *et al*., we concluded that there was not an association between trafficking and regulation
452 of migration upon EGF stimulation [21]. Upon further investigation of this cluster, we found several

453 sites that were shared with TGF-α cluster 1, such as the MAPK1/3/14 sites, EGFR_S991 and
454 EGFR_T693. We also found the inhibitory RAF1 site S259 and SCRIB_1448. SCRIB has a pu-
455 tative role in cell migration [45,46].

456 TGF-α clusters 4 and 5 also highly rank terms related to intracellular trafficking. In the ORA
457 analysis (Figure 4D) cluster 4 was also enriched for "regulation of clathrin-dependent endocyto-
458 sis", corroborating this association. Of particular interest in cluster 4 are the EGFR (Y1110,
459 Y1125 and Y1197), CBL (Y700) and CBLB (Y665. Y763. Y889) sites. None of the CBL/CBLB
460 sites have roles described in PSP, but these proteins are known regulators of receptor in trafficking
461 via clathrin [47,48]. Moreover, EGFR_Y1110 and EGFR_Y1197 are both annotated to receptor inter-
462 nalization in PSP, as well as inducing cell motility. This is in line with "regulation of epithelial
463 cell migration" highly ranked in this cluster (Figure 4C). Taken together, this data indicates that
464 TGF cluster 4 sites may have an initial role in regulating receptor internalization and migration,
465 whilst the cluster 1 sites are regulating later parts of the process.

466 As a positive control for assignment of functions to clustered sites, sites annotated in PSP to the
467 function "cell growth, inhibited" were added as a "spike-in" cluster to the EGF and TGF-α data,
468 with sites already found in the data excluded from this new cluster. RWHN and ORA were then
469 applied as previously. We found that both RWHN and ORA could assign these sites to the function
470 "negative regulation of cell growth" (Figure 5A). However, ORA assigned 134 and 122 other
471 terms to the sites added to the EGF and TGF data respectively, whilst RWHN assigned a refined
472 list of 36 and 39 respectively (Figure 5B). This result suggests that RWHN assigns more specific
473 functions to each phosphorylated site. Indeed, for each of the investigated clusters, RWHN was
474 able to assign sites belonging to those clusters to functions that closely resemble those that have
475 been experimentally proven by Francavilla *et al*. or described in PSP. The ORA results, whilst not

476 inaccurate, assigned more generic biological functions and did not assign specific terms. These
477 results suggest the RWHN algorithm can distinguish between sites of known function and can
478 assign functional terms to differentially regulated phosphorylation sites that could be further in-
479 vestigated experimentally.
480

A

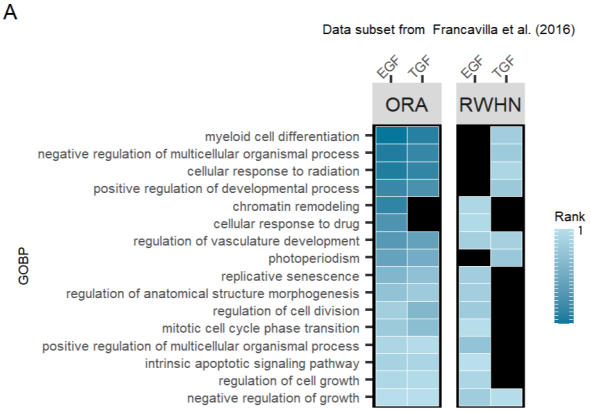

B

Data	Analysis	No. terms
EGF	ORA	134
TGF	ORA	122
EGF	RWHN	36
TGF	RWHN	29

Figure 5. Cluster containing sites annotated to "Cell growth, inhibited" in Phosphosite Plus, spiked into Francavilla et al. networks. A) Terms in common between ORA and RWHN results with both the EGF and TGF-α networks. B) Total number of terms in the output of both types of analyses on both networks.

481

482 **Experimental Case study 2: Phosphorylation-dependent response to Lapatinib treat-**
483 **ment and resistance in breast cancer**

484 To verify the applicability of the algorithm with non-temporal shotgun phosphoproteomics data,
485 we applied it to the experimental dataset from Ruprecht *et al.* [22] describing changes in the phos-
486 phoproteome upon treatment with the breast cancer drug lapatinib in sensitive ('parental' BT-474)
487 or lapatinib-resistant (BT-474-J4) cells. The paper uncovered and experimentally validated the
488 role of several metabolic enzymes and signaling pathways that were driving lapatinib resistance

489 in breast cancer. In particular, proteins that form the spliceosome, those involved in glycolysis
490 and glycogen catabolism and PI3K/AKT/mTOR pathway members were differentially phosphor-
491 ylated in lapatinib-resistant cells compared to parental lapatinib-treated cells. Further details on
492 the experimental design and results from the publication can be found in Supplementary Table
493 S2.

494 We first constructed a multilayer heterogeneous network, as described in Experimental Proce-
495 dures, which included 1603 phosphorylated sites that showed significant changes in response to
496 lapatinib treatment in either the parental or resistant cell lines (Table 4). Data were grouped into
497 5 clusters (referred to as clusters 1 – 5) using the k-means method. The number of clusters to use
498 was determined using the elbow plot method [29](Figure S4A), confirming that 5 clusters were suf-
499 ficient to capture all features found in the data. Indeed, sites sharing similar regulation profiles
500 between the resistant and parental cells were clustered together (Figure S4B). As the original pub-
501 lication used KEGG pathways rather than GO terms, we incorporated these in the functional-
502 annotation layer of our network to investigate the flexibility of our approach.

503

504 Table 4. Multilayer heterogeneous network, constructed from Ruprecht *et al.* [22] lapatinib-regu-
505 lated phosphorylated sites in parental and lapatinib-resistant cell lines. KEGG pathways were in-
506 cluded as functional annotations.

Subnetwork	Edges	Nodes
Site-site	75688	1599
Protein-protein	12752	3129
Function-function	15	152
Site-protein	1599	1599 sites, 930 proteins
Protein-function	692	103 proteins, 152 pathways

507

508 The results of RWHN applied to the multilayer heterogeneous network (Figure 6A) show that
509 when the seed nodes are set to sites belonging to cluster 4, representing sites that are less phos-
510 phorylated in lapatinib-resistant cells, the spliceosome pathway was highly ranked. This cluster
511 interestingly contained signalling sites such as ERBB2_Y1233, ERBB2_T1227, ERBB2_Y1233,
512 ERBB3_S627 and MAPK1_Y187, alongside sites on known spliceosome factors such as SRRM2
513 (S454, S2449), SRSF6 (S301) CWC25 (S170). Figure 6B shows that there was no enrichment for
514 any pathways in this cluster using standard ORA. However, ORA did show enrichment for meta-
515 bolic terms in several clusters, unlike RWHN, despite this being one of the clear conclusions of
516 the original paper. Metabolic pathways were enriched in clusters 3 ("glycolysis / gluconeogene-
517 sis") and 5 ("central carbon metabolism in cancer") using ORA. Since much of the investigation
518 and experimental validation by Ruprecht *et al.* [22] was done on the sites found to be regulated only
519 in lapatinib-treated resistant cells, we investigated whether our approach could uncover more nu-
520 anced roles of sites within these datasets. We constructed a second network using only those sites
521 that were regulated in lapatinib-treated resistant cells (Table 5). These were grouped into four
522 clusters (referred to as clusters 1 – 4) by K-means clustering as before (Figure S4A,C) and KEGG
523 pathways were used again in the functional annotation layer.

524

525 Table 5. Multilayer heterogeneous network, constructed from Ruprecht *et al.* [22] lapatinib-regu-
526 lated phosphorylated sites in lapatinib-resistant cell line. KEGG pathways were included as func-
527 tional annotations.

Subnetwork	Edges	Nodes
Site-site	668491	1910
Protein-protein	14770	3880
Function-function	15	187
Site-protein	1910	1910 sites, 1087 proteins
Protein-function	874	96 proteins, 187 pathways

528

529

530 As described in Figure 6C, two sets of seed nodes (clusters 2 and 3, representing sites substan-
531 tially upregulated and downregulated, Figure S4C) tended to rank metabolic pathways more
532 highly ("starch and sucrose metabolism", "galactose metabolism", "pentose phosphate pathway",
533 "purine metabolism", "amino sugar and nucleotide sugar metabolism"). Cluster 3, along with
534 cluster 1 (representing moderately downregulated sites), ranked "spliceosome" highly. These ini-
535 tial interpretations indicate that using a specific subset of the regulated sites in the data yielded
536 more specific and functionally relevant terms being ranked highly by the RWHN algorithm. More-
537 over, only cluster 2 showed enrichment for any metabolic pathways using ORA (Figure 6D). As
538 this is a large cluster containing all the sites shown to be significantly upregulated in the resistant
539 cell line, there is a considerable amount of 'noise' in the ORA results. The enrichment of two
540 metabolic pathways ("glycolysis / gluconeogenesis" and "central carbon metabolism in cancer")
541 potentially corroborate the role of these sites as metabolism regulators, as indicated by RWHN.
542 This cluster contained several of the sites classified as metabolic drivers of the resistance

phenotype, such as ENO1_Y44, PKM_Y175, PDHA_S293/S300. Intriguingly, S17 on the diverse signalling regulator SRC is also found in this cluster; this site is annotated to induction of enzymatic activity in PSP.

Figure 6. Site-centric and gene-centric analysis of Ruprecht *et al.* [22] datasets. (A) RWHN results related to sites regulated by lapatinib in lapatinib-resistant and parental cell lines. (B) ORA results related to proteins modified by lapatinib in lapatinib-resistant and parental cell lines. (C) RWHN

551 results related to sites regulated by lapatinib in lapatinib-resistant cell lines only. (D) ORA results
552 related to proteins modified by lapatinib in lapatinib-resistant cell lines only.

553

554 A closer look at cluster 3 uncovered sites on spliceosome factors (RBMX_S58, CDK13_S525,
555 CWC25_S17) and known signaling proteins (ERBB2_Y1233, FGFR4_S505). A site on the adap-
556 tor protein IRS2 (S1176) was also found in this cluster; as a known player in glucose and lipid
557 metabolism [49]. This points towards the link between rewired signalling and metabolism investi-
558 gated by Ruprecht *et al.* [22]. It is also annotated to "metastatic potential" in PSP, indicating its
559 therapeutic potential. ORA also showed enrichment for "spliceosome" in cluster 1. Indeed, this
560 cluster contained several of the sites highlighted in the paper. For example, the known lapatinib
561 responsive sites SF3B2_S309 and SF3B1_T261 could be found in this cluster, alongside 17 of the
562 30 SRRM2 sites that were significantly regulated by lapatinib.

563 From the comparison of ORA and the RWHN method we have extracted meaningful associa-
564 tions between specific phosphorylated sites and their functions in driving lapatinib resistance. Our
565 algorithm also highlighted potential further sites, such as IRS2_S1176, compared to the ORA
566 method, that may serve as hubs or intersections of crosstalk between key signalling pathways and
567 the rewired metabolic processes. It can be noted that the RWHN output was substantially more
568 refined than the ORA output, with the conclusions of the original paper being captured in 14 terms
569 in our analysis of the sites regulated in resistance, as opposed to 51 using ORA.

570 **Experimental Case Study 3: Spatially resolved activity of HRAS.**

571 The final dataset we analyzed described immunoprecipitation (IP) samples, in order for us to
572 see if our algorithm would be useful for analyzing local as well as global phosphoproteomes. The
573 subcellular localization of signaling proteins has been established as crucial in regulating cascades

574 and cellular processes. There are now numerous methods that allow experimental biologists to
575 detect spatial effects of proteins and phosphorylation, for example through proximity labeling and
576 targeted proteomics[50,51]. Recent work by Santra *et al.* [23] took a similar approach to investigate the
577 differential roles of a mutant, constitutively active form of HRAS, HRASV12, at different subcel-
578 lular locations. HRASV12 constructs tagged with different signal peptides (targeting them to dif-
579 ferent subcellular locations) were stably transfected into HeLa cells; this allowed the authors to
580 collect multi-omic samples with endogenous HRAS, unlocalized HRASV12 and HRASV12 lo-
581 calized to either the plasma membrane in disordered membrane regions (DM) or lipid rafts (LR),
582 Golgi apparatus (GA) and endoplasmic reticulum (ER). Using this approach, it was confirmed
583 that the majority of HRASV12 activity is mediated from the plasma membrane, with ER- and GA-
584 localized HRASV12 involved in regulating some of HRASV12's role in cell survival. Further
585 details on the experimental design and results from the publication can be found in Supplementary
586 Table S2.

587 The phosphoproteomics data from this study were clustered using k-means clustering, with an
588 optimal cluster number of 6 determined using an elbow plot (Figure S5A,B). Table 6 describes
589 the properties of the multilayer network constructed with these clusters. The first three clusters
590 represented dynamics discussed in the original paper: cluster 1 represented phosphorylated events
591 of mutant HRAS regardless of localization (location-independent); cluster 4 represented HRAS
592 in the secretory pathway, at the ER and GA (ER/GA); cluster 6 represented HRAS at the plasma
593 membrane, in the DM or LR (DM/LR). As these experimental conditions were best characterized
594 in the original paper, downstream analysis focused on these three clusters.
595

Table 6. Multilayer heterogeneous network, constructed using regulated sites from the Santra *et al.* [23] dataset. GOBP terms were included as functional annotations.

Subnetwork	Edges	Nodes
Site-site	766	621
Protein-protein	7262	2163
Function-function	370	452
Site-protein	621	621 sites, 474 proteins
Protein-function	900	122 proteins, 442 functions

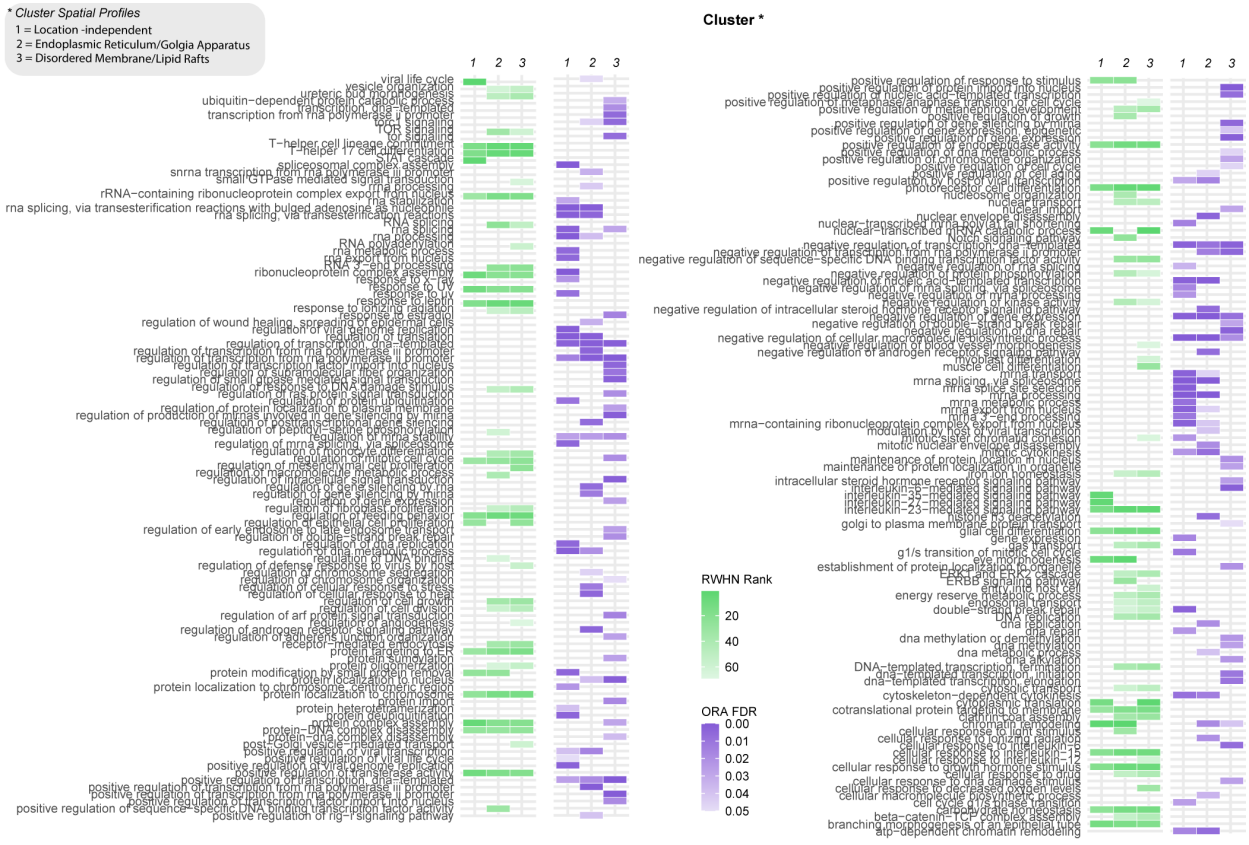

Figure 7. Site-centric and gene-centric analysis of Santra *et al.* [23] datasets; results from RWHN and ORA are in green and purple, respectively. Clusters shown in the figure refer to phosphorylated sites that are location-independent or found at the endoplasmic reticulum (ER)/Golgi

603 apparatus (GA) or disordered membrane (DM)/ lipid rafts (LR) (marked in the figure as clusters
604 1, 2, and 3, respectively).

605 Using RWHN (Figure 7, in purple), we found that the ER/GA and DM/LR clusters both highly
606 ranked key signaling pathways such as "ERK1 and ERK2 cascade" and "TOR signaling", along-
607 side signaling regulation such as "Receptor mediated endocytosis". This is consistent with the
608 finding from the original paper, that the majority of HRAS mediated effects derive from the lo-
609 calized population. Specifically, the DM/LR cluster ranks mitogenic processes highly, such as
610 "regulation of epithelial cell proliferation" and "positive regulation of metaphase/anaphase tran-
611 sition of cell cycle". The original paper also concluded that the majority of HRAS' mitogenic
612 effects were mediated from the plasma membrane. The ER/GA cluster independently ranks "pos-
613 itive regulation of growth" and "Notch signaling pathway". This potentially implicates ER/GA
614 localized HRAS, in the known developmental roles of HRAS in development; this was touched
615 upon but not investigated in the original paper.

616 Conversely, where a term is ranked highly in all three clusters, this could indicate that this is
617 part of the localization-independent regulation of HRAS. Twenty of the highly regulated terms fit
618 this definition; of these, several are related to immunological processes, such as T-help cell lineage
619 commitment" and "cellular response to interleukin-25". The location-independent cluster also in-
620 dependently ranks "interleukin-27-mediated signaling pathway" and "STAT cascade". This sug-
621 gests that HRAS' role in regulating cytokine and immune response is not location dependent.

622 An obvious outcome of the results using RWHN and ORA on this data is the difference in the
623 number terms associated to each cluster. There were 132 terms describing these clusters with ORA
624 (Figure 7, in green), compared to 86 with RWHN, with many of the enriched terms related to the
625 overrepresented categories depicted in Figure 3, such as "gene expression". Several comparisons

can be drawn between the results of the two analyses to add credence to the accuracy of results from RWHN. For example, cluster 1 shows enrichment for the term "Interleukin-6-mediated signaling pathway", and cluster 3 is enriched for the term "regulation of mitotic cell cycle". These results from ORA are consistent with the results from RWHN and the original paper, but with a significant amount of noise and redundancy in the ORA output relative to RWHN.

5. Discussion

Phosphorylation has an important impact on protein function and thus cellular behavior. Within a network of kinase-substrate interactions, phosphorylation modulates the flow of information and regulation of disparate processes throughout the cell. Understanding the impact of phosphorylation on protein function traditionally required the experimental investigation and manipulation of individual sites, however with the advent of high throughput phosphoproteomics thousands of novel phosphorylation sites of unknown function have been discovered. As there is limited experimentally validated information available on how regulation at individual phosphorylated sites impacts the downstream cellular output, current methods for analyzing high throughput phosphoproteomics data rely on general descriptors of phosphorylated protein function such as GO terms or involvement in known pathways. Their use in proteomics and transcriptomics analysis, though widespread, has come under recent criticism. Maertens *et al* [52] demonstrated that annotations are lacking for a substantial number of genes known to be important in cancer, whilst Haynes *et al*. [53] demonstrate a "rich-getting-richer" effect, with well-studied genes having higher annotation rates despite having less -omic or molecular evidence for the association with processes or diseases. These problems are exacerbated when used in analyzing phosphoproteomics data, as enrichment analyses also disregard site-specific or multiple-site regulation, masking the roles of proteins in a particular modification state [10,12].

650 Here, we developed and tested a method that associates phosphorylated sites to potential func-
651 tion using RWHN. By incorporating the pattern of phosphorylation upon perturbation, we con-
652 sider more of the information available in phosphoproteomics datasets and establish the phosphor-
653 ylated sites as the key drivers in the functional analysis. The algorithm is capable of recapturing
654 experimentally proven functions of phosphorylated sites in a non-gene centric manner, refining
655 analysis and extracting more information from phosphoproteomics data.

656 To prove the utility of our algorithm we applied it to a validation network, which represented a
657 simple model of phosphorylation dynamics in the MAPK/ERK pathway, and to two previously
658 published phosphoproteomics dataset describing temporal cellular signalling events and the im-
659 pact of resistance to drug treatment in breast cancer, respectively. Our algorithm successfully dis-
660 tinguished between differentially regulated phosphorylated sites from the same protein and asso-
661 ciated them to both known and previously uninvestigated functions. For example, when applying
662 this approach to the data from Francavilla *et al.* [21], we can recapture the roles of EGFR sites with
663 functions described in PSP. Both EGFR_Y1110 and EGFR_Y1197 are annotated to receptor in-
664 ternalization and cell motility in PSP; in our analysis, we found that these sites are both found in
665 clusters that associate with "regulation of clathrin dependent endocytosis", however only the TGF-
666 α cluster also ranked "regulation of cell migration" highly, reproducing the experimental evidence
667 from Francavilla *et al.* Whilst the authors of the original manuscript associated these sites with
668 their functions using a combination of gene-centric approaches and experimental validation, here
669 we use a single site-centric algorithm to extract these associations directly from the phosphopro-
670 teomics dataset, demonstrating the power of our approach in quickly and more specifically nar-
671 rowing down candidates for further functional studies. By associating ligand-dependent regulation

672 of phosphorylated sites, it is possible to disentangle their multifaceted role in regulating cellular
673 signalling networks and downstream cellular behaviors.

674 From the Ruprecht *et al*. data, we can use the example of SRRM2 to illustrate the validity of
675 our approach. This component of the spliceosome is known to be highly phosphorylated, with 675
676 phosphorylation sites recorded in PSP. At the time of writing none of these sites was ascribed to
677 a function in the database, despite the importance of phosphorylation and dephosphorylation
678 events in orchestrating splicing events [54]. It is also regularly mutated (>5% of cases in TGCA) in
679 lung, stomach, bladder, endometrial and colorectal cancers [6]. Ruprecht *et al*. uncovered a new role
680 for the spliceosome in modulating lapatinib-resistance, highlighting several sites on spliceosome
681 proteins (including SRRM2_S1132, S1987 and S970) that were differentially modified in resistant
682 and parental cell populations. Previous work has described how SRRM2-depletion in HER2-pos-
683 itive breast and ovarian cancer cells reduced the rate of migration [55]; the spliceosome plays myriad
684 roles in the breast cancer environment, but site-specific analysis is lacking. Using our algorithm,
685 we can begin to uncover the nuanced modification-specific roles of proteins such as SRRM2 in
686 metabolic rewiring. We suggest that eleven of the SRRM2 sites found in cluster 2 of the lapatinib-
687 resistant sites (Figure 6C) could be at the intersection between the spliceosome and metabolic
688 processes; the conjunction between these processes was central to the work of Ruprecht *et al*. The
689 sites in this cluster could be investigated as points of crosstalk between these different cellular
690 processes. This example highlights the value of our approach in generating hypotheses of modi-
691 fied protein function and signaling pathway crosstalk.

692 Although the associations predicted here between sites and functions cannot be interpreted as
693 causative, phosphorylation sites can act as indirect, and context-dependent, regulators in cellular
694 processes. This is demonstrated by the clustering of SRC_S17, a protein that is typically associated

695 with signalling downstream of cell-surface receptors, with a cluster that ranked metabolic path-
696 ways higher than cellular processing or signalling pathways. Critical to this is a robust method of
697 defining clusters, to capture meaningful regulatory patterns at different phosphorylated sites. Here
698 we define clusters using established techniques (e.g., elbow method for K-means) or visually iden-
699 tifying those with differing time-resolved behaviors. By using clusters to define edges between
700 phosphorylated sites in the multilayer heterogeneous network, the pattern of experimentally per-
701 turbed modules in the cellular system can be investigated. Although having fixed edges between
702 sites, as with the PPI layer of the multilayer network, would likely allow for a closer representation
703 of the whole cellular system, this would not be computationally viable nor in the interest of ex-
704 perimental biologists. This algorithm is targeted towards datasets that describe the effect of spe-
705 cific treatments or perturbations, allowing for a focused view on the impacted processes to identify
706 candidates to investigate further. Quantitatively defining the edges between phosphorylated sites
707 based on the dataset collected also prevents the issues plaguing standard enrichments analyses as
708 discussed before; fixed edges, defined on information in databases or previously published data,
709 would almost certainly skew the analysis towards well studied phosphorylated sites and biological
710 processes.

711 Multilayer heterogeneous networks are increasingly being used to integrate 'omic data; here,
712 their use allows phosphoproteomics data to be incorporated with PPI networks and functional
713 annotations, overcoming the issue of considering phosphoproteomics data primarily on the protein
714 level. A potential drawback of our approach is the reliance on large semi-curated resources such
715 GO or STRING. For instance, different clusters may have many terms or pathways in common
716 given the involvement of many proteins in the same biological functions and the high proportion
717 of frequently used GO terms [56]. We theorize that this may be rectified if the data were clustered

into more groups, in order to capture more nuanced phosphorylation patterns. However, enrichment of non-specific terms or false positives remains an issue when analyzing high-throughput 'omics data by other commonly used methods too. By only including edges in the protein layer of the network with a STRING experimental confidence score of greater than 0.4 and only including non-redundant terms in the function layer we have reduced the noise in the resulting list of associated terms. This could be taken further by filtering for only high confidence functional annotations or incorporating annotations from multiple sources into the network. Moreover, RWHN does not result in a different set of terms in the output compared to the accepted standard method ORA, but rather provides a refinement that will allow for biological insights to be reached more clearly.

Our method is flexible enough to be used with any discovery phosphoproteomics data that describes a change between conditions. This is an improvement on the previously published use of RWHN using multiple sources of phosphoproteomics data to uncover disease-dependent regulation [19]. Moreover, it could easily be generalized to any post-translational modification proteomics dataset, as it incorporates readily available PPI and functional annotation data, as demonstrated here. The fundamental aspect would be maintained with any of these expansions: specific patterns of regulation at modified sites dictate movement through the multilayer heterogeneous network.

6. Conclusion

We have proposed a site-centric approach to analyze phosphoproteomics data, that provides a robust alternative to gene-centric methods of analysis. We integrated clustered quantitative phosphoproteomics data, a context-specific PPI network and functional annotations into a multilayer, heterogeneous network and used the RWHN method to predict the functions of phosphorylation sites with similar regulatory patterns. Using our algorithm, we extracted experimentally validated

associations between phosphorylated sites and their role in cellular processes, which could not be captured using the typical gene-centric methods. Moreover, our algorithm has the potential to be used by researchers in predicting novel site-function associations and generating hypotheses to be experimentally validated.

7. Supporting Information

Figure S1. Optimization of RWHN parameters using the validation dataset.

Figure S2. Validation using randomly permuted networks.

Figure S3. Clustering of Francavilla et al. data.

Figure S4. Clustering of Ruprecht et al. data.

Figure S5. Clustering of Santra et al. data.

Table S1. PSP ON_PROCESS annotations, that describe biological function of sites, mapped to most closely related GOBP term.

Table S2. Summary of the experimental methods and results from each of the Case Study datasets.

Data and source code for the analysis described in the manuscript can be found at github.com/JoWatson2011/RWHN_Phosphoproteomics

An R package for use of the tool can be found at github.com/JoWatson2011/phosphoRWHN

8. Author Contributions

The manuscript was written through contributions of all authors. All authors have given approval to the final version of the manuscript.

9. Funding Sources

JW is supported by a Biotechnology and Biological Sciences Research Council (BBSRC) Doctoral Training Programme grant (BB/M011208/1). CF is supported by a Wellcome Trust Sir Henry Dale Fellowship (107636/Z/15/Z), the Biotechnology and Biological Sciences Research Council (BB/R015864/1), and the Medical Research Council (MR/T016043/1).

10. Acknowledgements

We would like to acknowledge the assistance given by Research IT and the use of the Computational Shared Facility at The University of Manchester. We would like to thank current and former members of the Schwartz and Francavilla labs for their thoughtful and insightful discussion on this work and Dr Joe Swift (University of Manchester) for useful comments on our manuscript.

11. Abbreviations

RWHN, Random walk on heterogeneous network; PTM, Post-translational modification; PPI, Protein-protein interaction; GO, Gene Ontology; PSP, Phosphosite Plus; EGF, Epidermal Growth Factor; TGF-α, Tumor growth factor α; RWR, Random walk with restart; GOBP, Gene Ontology Biological Processes; FDR, False discovery rate; SILAC, Stable Isotope Labelling of Amino Acids in Cell culture; KDE, Kernel Density Estimation

12. References

(1) Sugiyama, N.; Imamura, H.; Ishihama, Y. Large-Scale Discovery of Substrates of the Human Kinome. *Scientific Reports* **2019**, *9* (1), 10503. https://doi.org/10.1038/s41598-019-46385-4.

(2) Day, E. K.; Sosale, N. G.; Lazzara, M. J. Cell Signaling Regulation by Protein Phosphorylation: A Multivariate, Heterogeneous, and Context-Dependent Process. *Current Opinion in Biotechnology* **2016**, *40*, 185–192. https://doi.org/10.1016/j.copbio.2016.06.005.

(3) Vyse, S.; Desmond, H.; Huang, P. H. Advances in Mass Spectrometry Based Strategies to Study Receptor Tyrosine Kinases. *IUCrJ* **2017**, *4* (Pt 2), 119–130. https://doi.org/10.1107/S2052252516020546.

(4) Munk, S.; Refsgaard, J. C.; Olsen, J. V. Systems Analysis for Interpretation of Phosphoproteomics Data. In *Phospho-Proteomics: Methods and Protocols*; von Stechow, L., Ed.; Springer New York: New York, NY, 2016; pp 341–360. https://doi.org/10.1007/978-1-4939-3049-4_23.

(5) Sacco, F.; Perfetto, L.; Cesareni, G. Combining Phosphoproteomics Datasets and Literature Information to Reveal the Functional Connections in a Cell Phosphorylation Network. *PROTEOMICS* **2018**, *18* (5–6), 1700311. https://doi.org/10.1002/pmic.201700311.

(6) Hornbeck, P. V.; Zhang, B.; Murray, B.; Kornhauser, J. M.; Latham, V.; Skrzypek, E. PhosphoSitePlus, 2014: Mutations, PTMs and Recalibrations. *Nucleic Acids Research* **2015**, *43* (D1), D512–D520. https://doi.org/10.1093/nar/gku1267.

(7) Linding, R.; Jensen, L. J.; Pasculescu, A.; Olhovsky, M.; Colwill, K.; Bork, P.; Yaffe, M. B.; Pawson, T. NetworKIN: A Resource for Exploring Cellular Phosphorylation Networks. *Nucleic Acids Research* **2008**. https://doi.org/10.1093/nar/gkm902.

(8) Casado, P.; Rodriguez-Prados, J.-C.; Cosulich, S. C.; Guichard, S.; Vanhaesebroeck, B.; Joel, S.; Cutillas, P. R. Kinase-Substrate Enrichment Analysis Provides Insights into the Heterogeneity of Signaling Pathway Activation in Leukemia Cells. *Science signaling* **2013**, *6* (268), rs6. https://doi.org/10.1126/scisignal.2003573.

(9) Mischnik, M.; Sacco, F.; Cox, J.; Schneider, H.-C.; Schäfer, M.; Hendlich, M.; Crowther, D.; Mann, M.; Klabunde, T. IKAP: A Heuristic Framework for Inference of Kinase Activities from Phosphoproteomics Data. *Bioinformatics* **2016**, *32* (3), 424–431. https://doi.org/10.1093/bioinformatics/btv699.

(10) Needham, E. J.; Parker, B. L.; Burykin, T.; James, D. E.; Humphrey, S. J. Illuminating the Dark Phosphoproteome. *Science Signaling* **2019**, *12* (565), eaau8645. https://doi.org/10.1126/scisignal.aau8645.

(11) Rudolph, J. D.; de Graauw, M.; van de Water, B.; Geiger, T.; Sharan, R. Elucidation of Signaling Pathways from Large-Scale Phosphoproteomic Data Using Protein Interaction Networks. *Cell systems* **2016**, *3* (6), 585-593.e3. https://doi.org/10.1016/j.cels.2016.11.005.

(12) Krug, K.; Mertins, P.; Zhang, B.; Hornbeck, P.; Raju, R.; Ahmad, R.; Szucs, M.; Mundt, F.; Forestier, D.; Jane-Valbuena, J.; Keshishian, H.; Gillette, M. A.; Tamayo, P.; Mesirov, J. P.; Jaffe, J. D.; Carr, S. A.; Mani, D. R. A Curated Resource for Phosphosite-Specific Signature Analysis. *Molecular & cellular proteomics : MCP* **2019**, *18* (3), 576–593. https://doi.org/10.1074/mcp.TIR118.000943.

(13) Boyle, E. I.; Weng, S.; Gollub, J.; Jin, H.; Botstein, D.; Cherry, J. M.; Sherlock, G. GO::TermFinder—Open Source Software for Accessing Gene Ontology Information and Finding Significantly Enriched Gene Ontology Terms Associated with a List of Genes. *Bioinformatics* **2004**, *20* (18), 3710–3715. https://doi.org/10.1093/bioinformatics/bth456.

(14) Battiston, F.; Nicosia, V.; Chavez, M.; Latora, V. Multilayer Motif Analysis of Brain Networks. *Chaos: An Interdisciplinary Journal of Nonlinear Science* **2017**, *27* (4), 047404. https://doi.org/10.1063/1.4979282.

(15) Li, Y.; Patra, J. C. Genome-Wide Inferring Gene–Phenotype Relationship by Walking on the Heterogeneous Network. *Bioinformatics* **2010**, *26* (9), 1219–1224. https://doi.org/10.1093/bioinformatics/btq108.

(16) Jiang, R. Walking on Multiple Disease-Gene Networks to Prioritize Candidate Genes. *JOURNAL OF MOLECULAR CELL BIOLOGY* **2015**, *7* (3, SI), 214–230. https://doi.org/10.1093/jmcb/mjv008.

(17) Soul, J.; Hardingham, T. E.; Boot-Handford, R. P.; Schwartz, J.-M. PhenomeExpress: A Refined Network Analysis of Expression Datasets by Inclusion of Known Disease Phenotypes. *Scientific Reports* **2015**, *5* (1), 8117. https://doi.org/10.1038/srep08117.

(18) Tang, Y.; Chen, K.; Wu, X.; Wei, Z.; Zhang, S.-Y.; Song, B.; Zhang, S.-W.; Huang, Y.; Meng, J. DRUM: Inference of Disease-Associated M6A RNA Methylation Sites From a Multi-Layer Heterogeneous Network. *Frontiers in Genetics* **2019**, *10*, 266. https://doi.org/10.3389/fgene.2019.00266.

(19) Xu, X.; Wang, M. Inferring Disease Associated Phosphorylation Sites via Random Walk on Multi-Layer Heterogeneous Network. *IEEE/ACM Transactions on Computational Biology and Bioinformatics* **2016**, *13* (5), 836–844. https://doi.org/10.1109/TCBB.2015.2498548.

(20) Behar, M.; Hoffmann, A. Understanding the Temporal Codes of Intra-Cellular Signals. *Current Opinion in Genetics & Development* **2010**, *20* (6), 684–693. https://doi.org/10.1016/J.GDE.2010.09.007.

(21) Francavilla, C.; Papetti, M.; Rigbolt, K. T. G.; Pedersen, A.-K.; Sigurdsson, J. O.; Cazzamali, G.; Karemore, G.; Blagoev, B.; Olsen, J. V. Multilayered Proteomics Reveals Molecular Switches Dictating Ligand-Dependent EGFR Trafficking. *Nature Structural & Molecular Biology* **2016**, *23* (6), 608–618. https://doi.org/10.1038/nsmb.3218.

(22) Ruprecht, B.; Zaal, E. A.; Zecha, J.; Wu, W.; Berkers, C. R.; Kuster, B.; Lemeer, S. Lapatinib Resistance in Breast Cancer Cells Is Accompanied by Phosphorylation-Mediated Reprogramming of Glycolysis. *Cancer Research* **2017**, *77* (8), 1842–1853. https://doi.org/10.1158/0008-5472.CAN-16-2976.

(23) Santra, T.; Herrero, A.; Rodriguez, J.; von Kriegsheim, A.; Iglesias-Martinez, L. F.; Schwarzl, T.; Higgins, D.; Aye, T.-T.; Heck, A. J. R.; Calvo, F.; Agudo-Ibáñez, L.; Crespo, P.; Matallanas, D.; Kolch, W. An Integrated Global Analysis of Compartmentalized HRAS Signaling. *Cell reports* **2019**, *26* (11), 3100-3115.e7. https://doi.org/10.1016/j.celrep.2019.02.038.

(24) Cox, J.; Mann, M. MaxQuant Enables High Peptide Identification Rates, Individualized p.p.b.-Range Mass Accuracies and Proteome-Wide Protein Quantification. *Nature Biotechnology* **2008**, *26* (12), 1367–1372. https://doi.org/10.1038/nbt.1511.

(25) Tyanova, S.; Temu, T.; Sinitcyn, P.; Carlson, A.; Hein, M. Y.; Geiger, T.; Mann, M.; Cox, J. The Perseus Computational Platform for Comprehensive Analysis of (Prote)Omics Data. *Nature Methods* **2016**, *13* (9), 731–740. https://doi.org/10.1038/nmeth.3901.

(26) Ritchie, M. E.; Phipson, B.; Wu, D.; Hu, Y.; Law, C. W.; Shi, W.; Smyth, G. K. Limma Powers Differential Expression Analyses for RNA-Sequencing and Microarray Studies. *Nucleic Acids Research* **2015**, *43* (7), e47–e47. https://doi.org/10.1093/nar/gkv007.

(27) Schwämmle, V.; Jensen, O. N. A Simple and Fast Method to Determine the Parameters for Fuzzy c–Means Cluster Analysis. *Bioinformatics* **2010**, *26* (22), 2841–2848. https://doi.org/10.1093/bioinformatics/btq534.

(28) Campello, R. J. G. B.; Hruschka, E. R. A Fuzzy Extension of the Silhouette Width Criterion for Cluster Analysis. *Fuzzy Sets and Systems* **2006**, *157* (21), 2858–2875. https://doi.org/10.1016/J.FSS.2006.07.006.

(29) Zambelli, A. E. A Data-Driven Approach to Estimating the Number of Clusters in Hierarchical Clustering. *F1000Research* **2016**, *5*, 2809. https://doi.org/10.12688/f1000research.10103.1.

(30) Szklarczyk, D.; Gable, A. L.; Lyon, D.; Junge, A.; Wyder, S.; Huerta-Cepas, J.; Simonovic, M.; Doncheva, N. T.; Morris, J. H.; Bork, P.; Jensen, L. J.; Mering, C. von. STRING V11: Protein–Protein Association Networks with Increased Coverage, Supporting Functional Discovery in Genome-Wide Experimental Datasets. *Nucleic Acids Research* **2018**, *47* (D1), D607–D613. https://doi.org/10.1093/nar/gky1131.

(31) Yu, G.; Li, F.; Qin, Y.; Bo, X.; Wu, Y.; Wang, S. GOSemSim: An R Package for Measuring Semantic Similarity among GO Terms and Gene Products. *Bioinformatics* **2010**, *26* (7), 976–978. https://doi.org/10.1093/bioinformatics/btq064.

(32) Wang, J. Z.; Du, Z.; Payattakool, R.; Yu, P. S.; Chen, C.-F. A New Method to Measure the Semantic Similarity of GO Terms. *Bioinformatics* **2007**, *23* (10), 1274–1281. https://doi.org/10.1093/bioinformatics/btm087.

(33) Stoney, R. A.; Ames, R. M.; Nenadic, G.; Robertson, D. L.; Schwartz, J.-M. Disentangling the Multigenic and Pleiotropic Nature of Molecular Function. *BMC systems biology* **2015**, *9 Suppl 6* (Suppl 6), S3. https://doi.org/10.1186/1752-0509-9-S6-S3.

(34) Blondel, V. D.; Guillaume, J.-L.; Lambiotte, R.; Lefebvre, E. Fast Unfolding of Communities in Large Networks. *J. Stat. Mech.* **2008**, *2008* (10), P10008. https://doi.org/10.1088/1742-5468/2008/10/P10008.

(35) Kuleshov, M. V; Jones, M. R.; Rouillard, A. D.; Fernandez, N. F.; Duan, Q.; Wang, Z.; Koplev, S.; Jenkins, S. L.; Jagodnik, K. M.; Lachmann, A.; McDermott, M. G.; Monteiro, C. D.; Gundersen, G. W.; Ma'ayan, A. Enrichr: A Comprehensive Gene Set Enrichment Analysis Web Server 2016 Update. *Nucleic Acids Research* **2016**, *44* (W1), W90–W97. https://doi.org/10.1093/nar/gkw377.

(36) Carlson, M. GO.Db: A Set of Annotation Maps Describing the Entire Gene Ontology. R Package Version 3.8.2. *Bioconductor 3.10*. 2019.

(37) Köhler, S.; Bauer, S.; Horn, D.; Robinson, P. N. Walking the Interactome for Prioritization of Candidate Disease Genes. *The American Journal of Human Genetics* **2008**, *82* (4), 949–958. https://doi.org/10.1016/J.AJHG.2008.02.013.

(38) Riley, N. M.; Coon, J. J. Phosphoproteomics in the Age of Rapid and Deep Proteome Profiling. *Analytical Chemistry* **2016**, *88* (1), 74–94. https://doi.org/10.1021/acs.analchem.5b04123.

(39) Blatti, C.; Sinha, S. Characterizing Gene Sets Using Discriminative Random Walks with Restart on Heterogeneous Biological Networks. *Bioinformatics* **2016**, *32* (14), 2167–2175. https://doi.org/10.1093/bioinformatics/btw151.

(40) Shieh, G. S. A Weighted Kendall's Tau Statistic. *Statistics & Probability Letters* **1998**, *39* (1), 17–24. https://doi.org/10.1016/S0167-7152(98)00006-6.
(41) Fey, D.; Croucher, D. R.; Kolch, W.; Kholodenko, B. N. Crosstalk and Signaling Switches in Mitogen-Activated Protein Kinase Cascades. *Frontiers in Physiology* **2012**, *3*. https://doi.org/10.3389/fphys.2012.00355.
(42) Arkun, Y.; Yasemi, M. Dynamics and Control of the ERK Signaling Pathway: Sensitivity, Bistability, and Oscillations. *PLOS ONE* **2018**, *13* (4), e0195513. https://doi.org/10.1371/journal.pone.0195513.
(43) H. B. Mann; D. R. Whitney. On a Test of Whether One of Two Random Variables Is Stochastically Larger than the Other. *The Annals of Mathematical Statistics* **1947**, *18* (1), 50–60. https://doi.org/10.1214/aoms/1177730491.
(44) Benjamini, Y.; Hochberg, Y. Controlling the False Discovery Rate: A Practical and Powerful Approach to Multiple Testing. *Journal of the Royal Statistical Society: Series B (Methodological)* **1995**, *57* (1), 289–300. https://doi.org/10.1111/j.2517-6161.1995.tb02031.x.
(45) Dow, L. E.; Elsum, I. A.; King, C. L.; Kinross, K. M.; Richardson, H. E.; Humbert, P. O. Loss of Human Scribble Cooperates with H-Ras to Promote Cell Invasion through Deregulation of MAPK Signalling. *Oncogene* **2008**, *27* (46), 5988–6001. https://doi.org/10.1038/onc.2008.219.
(46) Nola, S.; Sebbagh, M.; Marchetto, S.; Osmani, N.; Nourry, C.; Audebert, S.; Navarro, C.; Rachel, R.; Montcouquiol, M.; Sans, N.; Etienne-Manneville, S.; Borg, J. P.; Santoni, M. J. Scrib Regulates PAK Activity during the Cell Migration Process. *Human Molecular Genetics* **2008**, *17* (22), 3552–3565. https://doi.org/10.1093/hmg/ddn248.
(47) Pennock, S.; Wang, Z. A Tale of Two Cbls: Interplay of c-Cbl and Cbl-b in Epidermal Growth Factor Receptor Downregulation. *Molecular and Cellular Biology* **2008**, *28* (9), 3020–3037. https://doi.org/10.1128/mcb.01809-07.
(48) Roepstorff, K.; Grandal, M. V.; Henriksen, L.; Knudsen, S. L. J.; Lerdrup, M.; Grøvdal, L.; Willumsen, B. M.; Van Deurs, B. Differential Effects of EGFR Ligands on Endocytic Sorting of the Receptor. *Traffic* **2009**, *10* (8), 1115–1127. https://doi.org/10.1111/j.1600-0854.2009.00943.x.
(49) Neukamm, S. S.; Toth, R.; Morrice, N.; Campbell, D. G.; MacKintosh, C.; Lehmann, R.; Haering, H. U.; Schleicher, E. D.; Weigert, C. Identification of the Amino Acids 300-600 of IRS-2 as 14-3-3 Binding Region with the Importance of IGF-1/Insulin-Regulated Phosphorylation of Ser-573. *PLoS ONE* **2012**, *7* (8). https://doi.org/10.1371/journal.pone.0043296.
(50) Gingras, A.-C.; Abe, K. T.; Raught, B. Getting to Know the Neighborhood: Using Proximity-Dependent Biotinylation to Characterize Protein Complexes and Map Organelles. *Current Opinion in Chemical Biology* **2019**, *48*, 44–54. https://doi.org/10.1016/j.cbpa.2018.10.017.
(51) Orre, L. M.; Vesterlund, M.; Pan, Y.; Arslan, T.; Zhu, Y.; Fernandez Woodbridge, A.; Frings, O.; Fredlund, E.; Lehtiö, J. SubCellBarCode: Proteome-Wide Mapping of Protein Localization and Relocalization. *Molecular Cell* **2019**, *73* (1), 166-182.e7. https://doi.org/10.1016/j.molcel.2018.11.035.
(52) Maertens, A.; Tran, V. P.; Maertens, M.; Kleensang, A.; Luechtefeld, T. H.; Hartung, T.; Paller, C. J. Functionally Enigmatic Genes in Cancer: Using TCGA Data to Map the Limitations of Annotations. *Scientific reports* **2020**, *10* (1), 4106. https://doi.org/10.1038/s41598-020-60456-x.

(53) Haynes, W. A.; Tomczak, A.; Khatri, P. Gene Annotation Bias Impedes Biomedical Research. *Scientific Reports* **2018**, *8* (1), 1362. https://doi.org/10.1038/s41598-018-19333-x.
(54) Naro, C.; Sette, C. Phosphorylation-Mediated Regulation of Alternative Splicing in Cancer. *International Journal of Cell Biology*. 2013. https://doi.org/10.1155/2013/151839.
(55) Mukherji, M.; Brill, L. M.; Ficarro, S. B.; Hampton, G. M.; Schultz, P. G. A Phosphoproteomic Analysis of the ErbB2 Receptor Tyrosine Kinase Signaling Pathways. *Biochemistry* **2006**, *45* (51), 15529–15540. https://doi.org/10.1021/bi060971c.
(56) Gaudet, P.; Dessimoz, C. Gene Ontology: Pitfalls, Biases, and Remedies. In *The Gene Ontology Handbook*; Dessimoz, C., Škunca, N., Eds.; Springer New York: New York, NY, 2017; pp 189–205. https://doi.org/10.1007/978-1-4939-3743-1_14.

For table of contents only
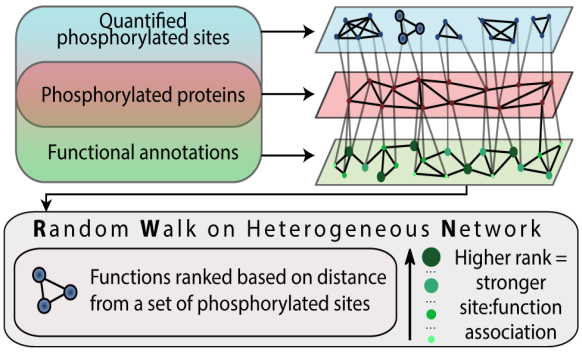
We confirm that the eTOC figure contains original material drawn by the authors.